

Restoration of Motor Function Through Delayed Intraspinal Delivery of Human IL-10-Encoding Nucleoside-Modified mRNA After Spinal Cord Injury

hIL-10 mRNA-Induced Restoration of Spinal Cord Function

László Gál¹, Tamás Bellák¹, Annamária Marton², Zoltán Fekécs¹, Drew Weissman³, Dénes Török¹, Rachana Biju¹, Csaba Vizler², Rebeka Kristóf¹, Mitchell B. Beattie⁴, Paulo J.C. Lin⁴, Norbert Pardi³, Antal Nógrádi^{1*}, Krisztián Pajer¹

¹Department of Anatomy, Histology and Embryology, Albert Szent-Györgyi Medical School, University of Szeged, Szeged, Hungary

²National Biotechnology Laboratory, Institute of Genetics, Biological Research Center, Szeged, Hungary

³Department of Medicine, University of Pennsylvania, Philadelphia, 19104, Pennsylvania, USA

⁴Acuitas Therapeutics, Vancouver, BC, V6T 1Z3, Canada

Corresponding author: Antal Nógrádi; nogradi.antal@med.u-szeged.hu.

Abstract

Efficient *in vivo* delivery of anti-inflammatory proteins to modulate the microenvironment of an injured spinal cord and promote neuroprotection and functional recovery is a great challenge. Nucleoside-modified messenger RNA (mRNA) has become a promising new modality that can be utilized for the safe and efficient delivery of therapeutic proteins. Here, we used lipid nanoparticle (LNP)-encapsulated human (h)IL-10-encoding nucleoside-modified mRNA to induce neuroprotection and functional recovery following rat spinal cord contusion injury. Intralesional administration of hIL-10 mRNA-LNP to rats led to a remarkable reduction of the microglia/macrophage reaction in the injured spinal segment and induced significant functional recovery compared to controls. Furthermore, hIL-10 mRNA treatment induced increased expression in TIMP-1 and CNTF levels in the affected spinal segment indicating a time-delayed secondary effect of IL-10 five days after injection. Our results suggest that treatment with nucleoside-modified mRNAs encoding neuroprotective factors is an effective strategy for spinal cord injury repair.

1. Introduction

Traumatic spinal cord injury affects nearly 1.4 million North Americans, many of whom are younger than 30 years old (1). SCI is a devastating disorder leading to loss of both grey and white matter and disrupts the connection the brain and rostral spinal cord from the caudal parts of the cord (2). After the primary injury, number of neurons and glia cells die within days in the lesion area resulting in permanent, incurable functional deficits. Many of these injuries affect the long ascending and descending tracts thus separating the lower spinal cord segments from the higher motor and sensory centres (3). After the primary physical injury, the number of process begins called secondary injury, the extent of which is always larger than that of the primary injury (1). Due to this phase, second set of symptoms can be observed in the injured spinal cord such as apoptosis, glutamate excitotoxicity, disruption of the blood-brain barrier, demyelination and reactive astrogliosis (4). Taken together these processes induce extensive scar formation, Wallerian degeneration and cavity formation (2-4).

Administration of interleukin-10 (IL-10) protein has shown promise in the treatment/cure of SCI, but safe and efficient drug delivery to the injured spinal cord represents an elusive goal. Several studies have demonstrated that administration or induced expression of IL-10 protein following experimental spinal cord injury improved neuronal survival and a certain level of functional recovery (5, 6).

However, the short half-life of IL-10 and its instability in circulation represents a major challenge, necessitating repeated or continuous administration. Several strategies have been developed for the reliable delivery of neurotrophic factors or cytokines to injured spinal cord but these approaches are often invasive and associated with adverse effects (5, 7, 8). These delivery approaches have included viral vectors, repeated intrathecal/intravenous injections and the use of osmotic pumps (5, 8, 9). Therefore, development of a safe and controllable tool for

cytokine delivery where the combined action of the identified biomolecules elicit definite morphological and functional improvement is critically important.

Messenger RNA (mRNA)-based therapy has recently emerged as a safe and very efficient approach that has wide applicability ranging from vaccination through protein replacement to gene editing (10-14). mRNA-based therapy has several conceptual advantages over protein or other nucleic acid-based approaches. These advantages include the lack of insertional mutagenesis, continued production of the required protein for days and no need of nuclear entry for the mRNA molecules. The most advanced mRNA delivery platform utilizes lipid nanoparticle (LNP)-encapsulated nucleoside-modified mRNA. Modification of the mRNA is critical to reduce inflammatory responses after mRNA delivery and increase protein production from mRNA (15, 16). LNP serves as an efficient carrier molecule for in vivo mRNA delivery, protecting the mRNA from rapid degradation and facilitating its cellular uptake. In this study, we utilized a human (h)IL-10-encoding mRNA-LNP construct for the treatment of injured spinal cords in a rat model system.

The aim of this study was to investigate whether intraspinally applied nucleoside-modified hIL-10 mRNA-LNP was able to be transiently translated in the injured spinal cord and induce significant neuroprotection and locomotor recovery. Our results may open new avenues for mRNA-mediated gene transfer to improve the outcome of spinal cord injuries by precisely modulating protein expression by the host cells of the injured cord.

2. Results

2.1. Intraspinal delivery of eGFP mRNA-LNP results in transient protein production in the intact spinal cord

Recent findings from our laboratories showed that a single injection of low doses of LNP-formulated firefly luciferase-encoding mRNA (0.1-5 μg) resulted in high levels of protein production for up to 10 days depending on the dose and the site of delivery in mice (17). To examine the duration and distribution of protein production from mRNA-LNP in the central nervous system, 3 μg of eGFP mRNA-LNP was pressure-injected into the intact rat spinal cord at the T10 vertebral level on day 0 (Supplement. Fig. 1a). Strong immunofluorescent signal was observed rostrally and caudally from the injection site for 5 days after injection (Fig. 1a and b). The highest amount of eGFP expression was detected 1 day after injection and then a decreasing field of eGFP signal could be measured for up to 21 days (Fig. 1c), when GFP expression was restricted to a very small area around the injection site. The eGFP protein was mainly detected in GFAP-positive astrocytes and TUBB3-positive neurons in the affected segment, resulting in colocalization areas of eGFP/GFAP ($22.5\pm 10.3\%$, S.E.M) and eGFP/TUBB3 ($29\pm 4.8\%$, S.E.M, Fig. 1d, f). As an extra cell population, GSA-B4-positive microglia/macrophages expressed eGFP along the injection channel only on day 1 after injection (Fig. 1e, eGFP/GSA-B4 colocalization area: $25\pm 7.5\%$, S.E.M). Iba-1, a microglia marker also colocalized with eGFP in microglia cells (eGFP/Iba-1 colocalization area: $5.8\pm 1.3\%$, S.E.M, Supplement. Fig. 3). eGFP was produced only by astrocytes and neurons 2 and 5 days after the mRNA-LNP administration (colocalization areas of eGFP/GFAP and eGFP/TUBB3 on day 2: $12.1\pm 4\%$ and $19\pm 10.4\%$, S.E.M, on day 5: $29.7\pm 5.1\%$ and $12.4\pm 1\%$, S.E.M., Supplement. Fig. 2a-f). At later time points eGFP expression of neurons ceased as it was maintained only in astrocytes up to

day 21 (colocalization area of eGFP/GFAP on day 9: $18.6 \pm 7.2\%$, S.E.M, on day 14: $15.3 \pm 5.8\%$, S.E.M.; on day 21: $14.3 \pm 6.3\%$, S.E.M.; Supplement. Fig. 2g-o).

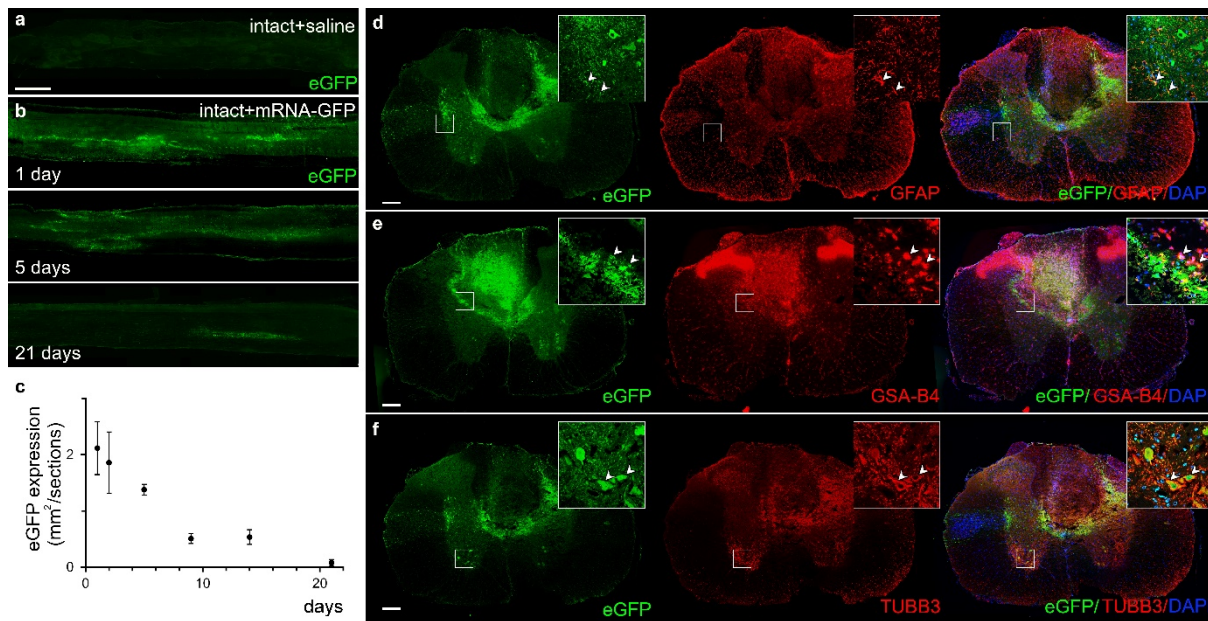


Figure 1. eGFP expression in intact rat spinal cords following intraspinal delivery of mRNA-LNP encoding eGFP. a) No eGFP expression can be seen in the intact rat spinal cord without intraspinal administration of mRNA-LNP encoding eGFP. **b)** eGFP expression in parasagittal sections of rat spinal cord 1, 5 and 21 days after the intraspinal injection of mRNA-LNP. The extent of eGFP positive area is very limited 21 days after mRNA-LNP administration. **c)** Quantification of the fluorescent eGFP signal after intraspinal injection of 3.0 µg mRNA-LNP. Note the marked drop in the size of eGFP+ area after 5 days. **d-e)** Cross sections of spinal cord show immunohistochemically detected eGFP in astrocytes (GFAP+) (**d**), in neurons (TUBB3+) (**e**) and in microglia/macrophages (GSA-B4+) (**f**) 1 day after the intraspinal mRNA-LNP administration. Data represent the mean \pm S.E.M in **c** (n=4; biologically independent experiments). Arrowheads show the co-localized cells. Scale bars in **a**=1 mm, in **d-f**=200 µm.

2.2. Protein expression after delayed intralesional delivery of eGFP-mRNA-LNP in the injured spinal cord

We next examined the expression kinetics of protein production from eGFP mRNA-LNP in injured spinal cords (*mRNA-GFP group*). Strong eGFP immunofluorescent signal was detected at the lesion site and rostrally and caudally from the end of the lesion cavity following intralesional delivery of mRNA-LNP encoding eGFP (Fig. 2b). The greatest area of eGFP expression was measured at 1 day after the injection of mRNA-LNP followed by a slow decrease in protein production up to 21 days (Fig. 2b). To determine the cell types transfected by eGFP mRNA-LNP, paramedian sagittal spinal cord tissue sections were mapped for eGFP co-labelling with GFAP (astrocytes), TUBB3 (neurons), GSA-B4 (microglia/macrophages) and Iba-1 (microglia). Up to day 5 after injection eGFP/GFAP-positive astrocytes, eGFP/GSA-B4-positive microglia/macrophages and eGFP/Iba-1-positive microglia cells were detected mainly around the lesion site (colocalization area of eGFP/GFAP on day 1: $41.6 \pm 13.4\%$, S.E.M.; colocalization area of eGFP/GSA-B4 on day 1: $42.9 \pm 3.6\%$, S.E.M.; colocalization area of eGFP/Iba-1 on day 1: $22.8 \pm 4.1\%$, S.E.M, colocalization area of eGFP/GFAP on day 2: $42.1 \pm 1.8\%$, S.E.M, colocalization area of eGFP/GSA-B4 on day 2: $26.9 \pm 3.8\%$, S.E.M.; colocalization area of eGFP/Iba-1 on day 2: $27.8 \pm 6.5\%$, S.E.M; colocalization area of eGFP/GFAP on day 5: $32.7 \pm 2.2\%$, S.E.M; colocalization area of eGFP/GSA-B4 on day 5: $12 \pm 1.8\%$, S.E.M.; colocalization area of eGFP/Iba-1 on day 5: $15.2 \pm 3.3\%$, S.E.M; Fig. 2d-f, 2j-l, Supplement. Fig. 4a, b, Supplement Fig. 5a-c) while rostrally and caudally from the lesion, a number of TUBB3-positive neurons and their processes expressed strongly eGFP (colocalization area of eGFP/TUBB3 on day 1: $40.5 \pm 2.5\%$, S.E.M; colocalization area of eGFP/TUBB3 on day 2: $32.3 \pm 12.9\%$ S.E.M; colocalization area of eGFP/TUBB3 on day 5: $27.6 \pm 5.7\%$, S.E.M; Fig. 2g-i, Supplement Fig. 4a, b). On days 9 and 14 after mRNA-LNP injection, only neurons and astrocytes showed eGFP expression (colocalization areas of

eGFP/GFAP on days 9 and 14: $31.7\pm 5.2\%$, S.E.M and $20.3\pm 3.7\%$, S.E.M; colocalization area of eGFP/TUBB3 on days 9 and 14: $16.7\pm 3.6\%$, S.E.M and $8.3\pm 4.8\%$. S.E.M, Supplement. Fig. 4c-e; Supplement Fig. 5d-f), while on day 21 exclusively few astrocytes showed co-localization with the eGFP protein (colocalization area of eGFP/GFAP on day 21: 11.8 ± 4.4 , S.E.M., Supplement Fig. 4f). These results clearly demonstrated that intralesional administration of mRNA-LNP into the injured spinal cord resulted in active and transient translation of mRNA to protein.

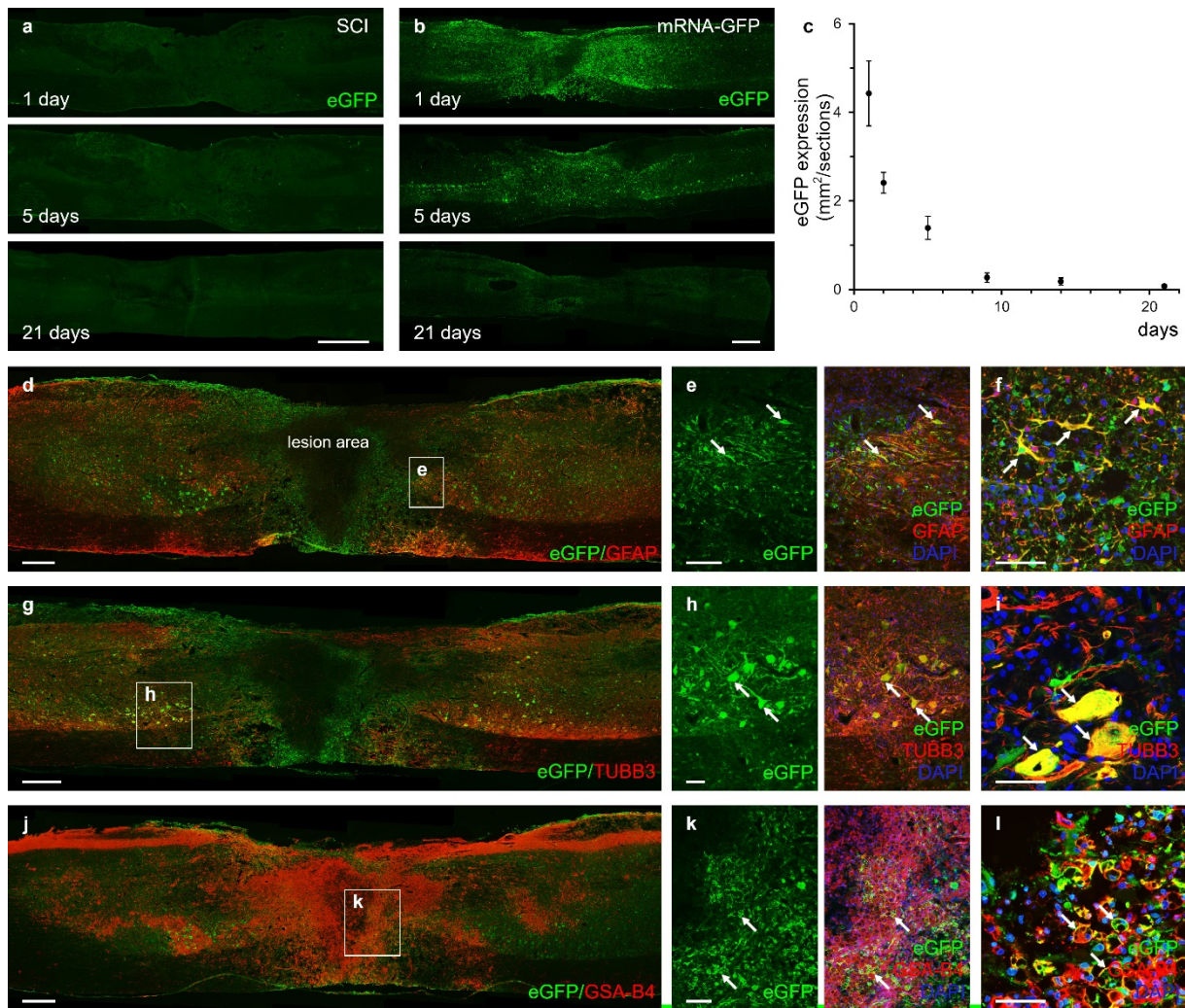


Figure 2. Protein production from eGFP mRNA-LNP in injured rat spinal cord after intralesional delivery. a) No eGFP expression is seen in the untreated SCI group. SCI animals received spinal cord contusion injury and 3 μ l saline 7 days after injury. **b)** eGFP expression in injured spinal cords followed up to 21 days after intraspinal mRNA-LNP encoding eGFP administration. **c)** Quantification of eGFP expression in parasagittal sections of spinal cords at various time points in the mRNA-GFP animals. The eGFP expression drops dramatically after 5 days. **d-l)** Astrocytes (GFAP+) (**d-f**), neurons (TUBB3+) (**g-i**) and microglia/macrophages (GSA-B4+) (**j-l**) expressed eGFP 1 day after intraspinal delivery of mRNA-LNP encoding eGFP. (**f, i** and **l**) Higher magnification clearly shows the presence of eGFP in the cytoplasm of astrocytes, neurons and microglia/macrophages. Arrows show GFAP, TUBB3 and GSA-B4-

positive cells co-localizing eGFP. Data represent the mean \pm S.E.M in **c** (n=4; biologically independent experiments). Scale bars in **a** and **b**=1 mm, in **d**, **g** and **j**=500 μ m, in **e**, **h**, **k**=100 μ m, in **f**, **i** and **l**=50 μ m.

2.3. Expression of hIL-10 mRNA-LNP in the injured spinal cord: kinetics and localization

Next the expression and synthesis of the anti-inflammatory hIL-10 was tested after delayed intralesional delivery of 3 μ g of hIL-10 mRNA-LNP following spinal cord contusion injury in rats (*mRNA-hIL-10 group*). Paramedian sagittal sections of the spinal cords were immunostained with hIL-10-specific antibody and strong immunofluorescence was detected rostrally and caudally from the injection site on days 1 and 2 and weak expression 5 days after the injection of hIL-10 mRNA-LNP (Fig. 3a-b). The ELISA results supported the immunohistochemical findings as high hIL-10 expression was detected on day 1 after the injection followed by a steady decline until day 5 in the injured spinal cord (Fig. 3c). Interestingly, hIL-10 was also detected in the blood serum 1 day after intralesional mRNA treatment, but at later time points only insignificant amounts of hIL-10 was detectable (Fig. 3d). On day 1 after mRNA-LNP injection, granular expression of hIL-10 could be observed in the cell body, but not in the processes of TUBB3-positive neurons in the affected segment (colocalization area of hIL-10/TUBB3: $7.5 \pm 1.6\%$, S.E.M, Fig. 3e-g).

hIL-10 was also found to be expressed in the astrocytes in the perilesional area (colocalization area of hIL-10/GFAP: $10.7 \pm 2.8\%$, S.E.M, Fig. 3h-j), while a number of GSA-B4-positive microglia/macrophages contained hIL-10-positive profiles at the interface between the lesion and preserved spinal cord (colocalization area of hIL-10/GSA-B4: $2.5 \pm 0.8\%$, S.E.M). Iba-1 also colocalizes in microglia with hIL-10 (colocalization area of hIL-10/Iba-1: $11.3 \pm 5.8\%$, S.E.M., Fig. 3k-m, Supplement. Fig. 6). Similar expression pattern of hIL-10 was noticed on day 2 after the mRNA delivery (colocalization areas of hIL-10/GFAP and hIL-10/TUBB3: $7.6 \pm 3.2\%$, S.E.M and $4.7 \pm 1.3\%$, S.E.M, Supplement. Fig. 7a). Five days after mRNA-LNP administration, hIL-10 protein expression was observed only in the soma of neurons and astrocytes in the close vicinity of the lesion (colocalization areas of hIL-10/GFAP and hIL-10/TUBB3: $5.8 \pm 1.9\%$, S.E.M and $2.9 \pm 2.7\%$, S.E.M, respectively, Supplement. Fig. 7b). In

contrast to the translation of eGFP mRNA-LNP in the injured spinal cord, hIL-10 expression was not detected 9 or 14 days after intralesional administration. These results suggest that the host cells of the spinal cord were transfected by the hIL-10 mRNA-LNP leading to active protein synthesis at least for 5 days, while the activated microglia/macrophages likely phagocytosed the already transfected cells.

In the case when osmotic pumps were used (*osm-hIL-10 group*) it was not possible to reliably determine the tissue level of IL-10 in the spinal cord or the further fate of delivered IL-10 in the spinal cord.

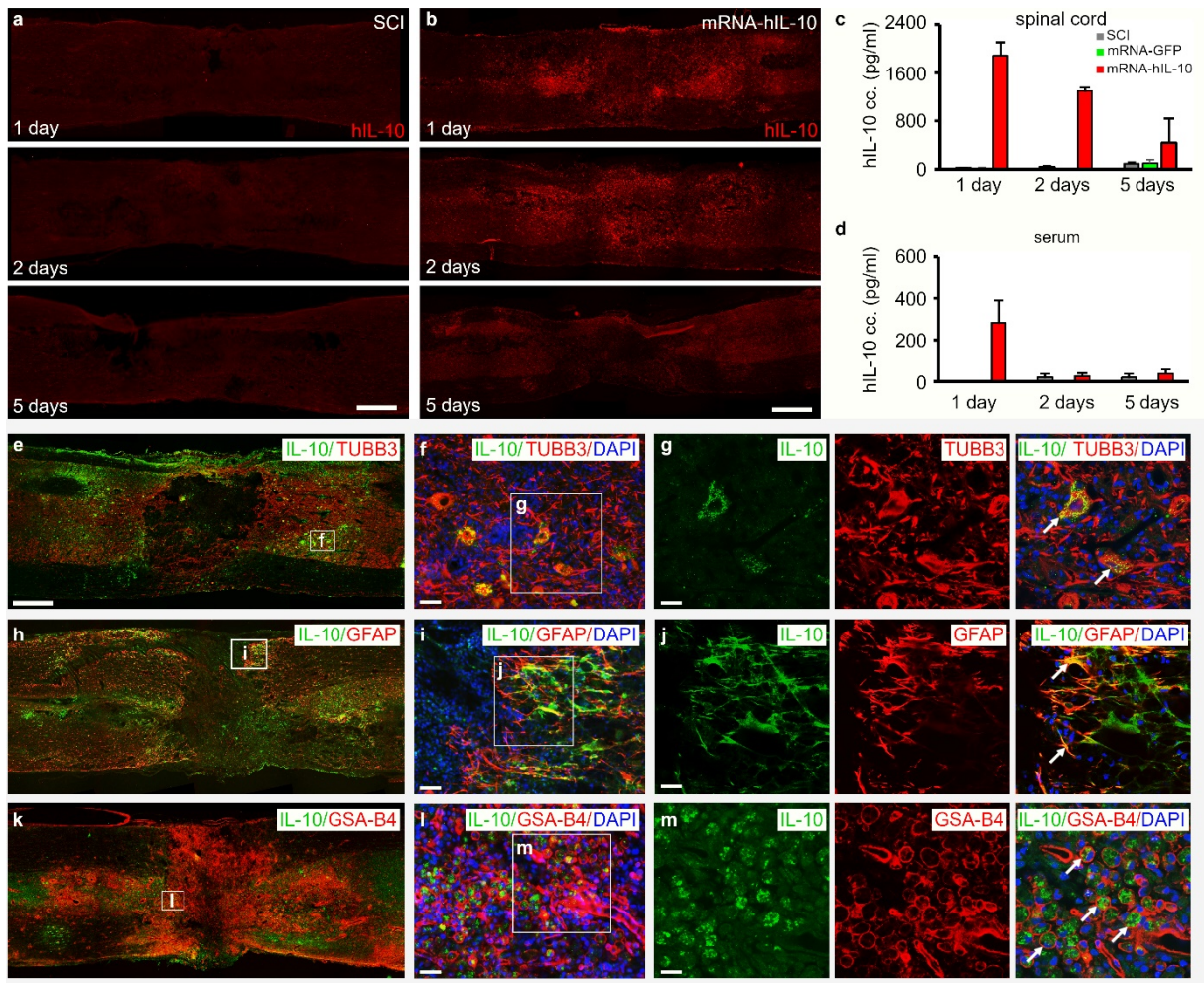


Figure 3. hIL-10 expression in injured spinal cords following intraslesional delivery of mRNA-LNP encoding hIL-10. a) No hIL-10 expression was detected in the injured rat spinal cord (SCI group). SCI animals received 3 μ l saline intraslesionally 7 days after the spinal cord contusion injury. **b)** hIL-10 expression detected in paramedian sagittal sections of injured rat spinal cords 1, 2 and 5 days after intraspinal delivery of mRNA-LNP encoding hIL-10. **c)** and **d)** Production of hIL-10 in injured spinal cord and serum after hIL-10 mRNA-LNP delivery determined by ELISA. **e-g)** Rat neurons express hIL-10 1 day after intraslesional mRNA-LNP administration. **h-j)** Rat astrocytes produced hIL-10 in the close vicinity of the lesion 1 day after mRNA-LNP delivery. **k-m)** GSA-B4 positive cells co-localized with hIL-10 in the lesion area 1 day after mRNA-LNP delivery. Data represent the mean \pm S.E.M; **c,d)** n=4, biologically

independent experiments. Arrows show the co-localized cells. Scale bar in **a** and **b**=800 μm , in **e**=750 μm , in **f** and **l**=30 μm , in **i** 25= μm and in **g**, **j**, **m**=20 μm .

2.4. Improved locomotor pattern after hIL-10 protein treatment via osmotic pump or mRNA-LNP delivery

To test the locomotor improvement after hIL-10 treatment through either the use of an osmotic pump to deliver the recombinant hIL-10 protein (*osm-hIL-10*) or by hIL-10 mRNA-LNP administration (mRNA-hIL-10) we used the BBB locomotor rating scale and the kinematic analysis developed in our laboratory (18, 19). From week 3 after injury, a notable improvement based on the BBB score was observed both in the *mRNA-hIL-10* and *osm-hIL-10* animals followed by a continuous motor improvement up to 9 weeks (Fig. 4a). In the *osm-hIL-10* group, animals showed similar locomotor pattern as *mRNA-hIL-10* treatment group, although mRNA-hIL-10 animals produced slightly, but non-significantly better BBB values than the animals that received IL-10 treatment via osmotic pumps. Statistically significant differences were found between the hIL-10 treated animals (*mRNA-hIL-10* and *osm-hIL-10* groups) and their controls (*SCI* and *mRNA-GFP* groups; $p \leq 0.05$; Fig 4a).

The kinematics analysis of IL-10-treated (*mRNA-hIL-10* and *osm-hIL-10* groups) and control rats (*SCI* and *mRNA-GFP* groups) was performed to provide quantitative information about knee flexion and lifting, ankle flexion and lifting, metatarsus surface angle and tibia surface angle at 9 weeks after the injury (Fig. 4b-d). Consistent with the BBB results (9 weeks after injury), the kinematic analysis revealed that hIL-10 treated animals (*mRNA-hIL-10* and *osm-hIL-10* group) displayed a significant improvement in all examined parameters compared to control animals (*SCI* and *mRNA-GFP* groups) that displayed only slight recovery after SCI.

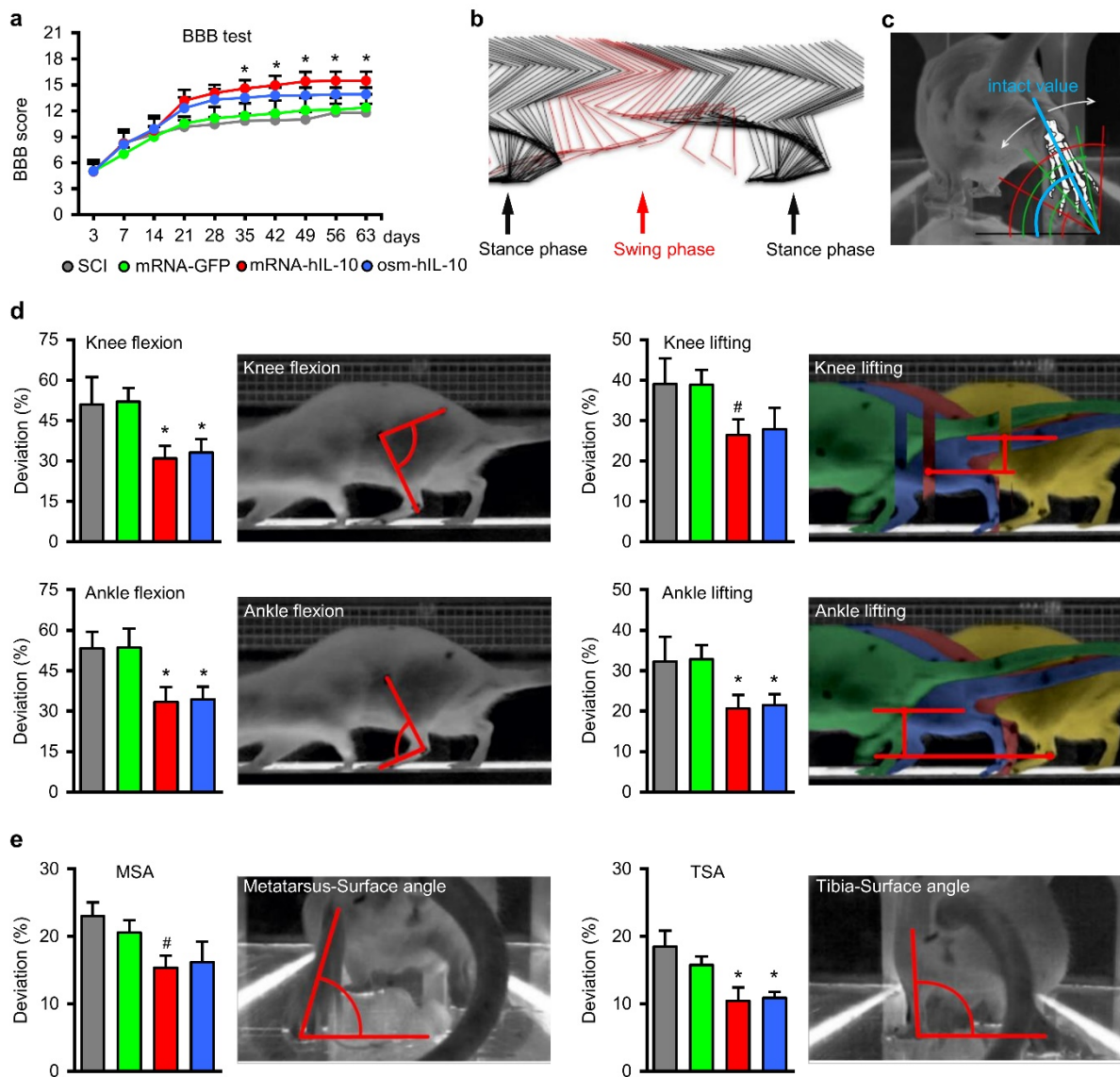


Figure 4. Delayed intraspinal administration of mRNA-LNP encoding hIL-10 improves locomotor function. **a)** Open field locomotor test (BBB) shows significant improvement of hIL-10 treated animals (mRNA-hIL-10 and osm-hIL-10 group) compared with their controls. Asterisks indicate significant difference between the hIL-10 treated animals (mRNA-hIL-10 and osm-hIL-10 group) and SCI and mRNA-GFP groups at various time points. **b)** The image shows every position of the measured bones during one intact step cycles from the lateral aspect. The step cycle can be divided into stance phase (black) and swing phase (red). **c)** The measurement of the rear-view parameters is based on the angle enclosed by a selected bone and

the floor plate. The intact value is displayed in blue, while green and red angles are representing the deviations followed by contusion injury, respectively. White arrows show the deviations in both directions. **d, e**) Kinematic analysis of the animals in the various groups 9 weeks after injury. Note the significantly improved parameters of the hIL-10 treated animals (mRNA-hIL-10 and osm-hIL-10 group) compared with SCI and mRNA-GFP groups. Data represent the mean \pm S.E.M. **a, d and e**) n=8, biologically independent experiments. * $p < 0.05$ and indicates significant difference among SCI, mRNA-GFP vs. mRNA-hIL-10 and osm-hIL-10 group. # $p < 0.05$ and shows significant difference between SCI, mRNA-GFP vs. mRNA-IL10 group. Data were analysed using the two-way ANOVA (**a**) or one-way ANOVA with LSD multiple comparisons tests (**d, e**).

2.5. Morphological restoration following intralesional delivery of mRNA-LNP encoding hIL-10

Morphometric analysis of the lesion area at the epicentre and spared tissue was performed 9 weeks after the injury. Within the lesion area a rostro-caudally extended cavity was observed with some cellular debris in SCI groups (Fig. 5a). Administration of hIL-10 (*mRNA-hIL-10* and *osm-hIL-10*) resulted in significantly smaller lesion area at the epicentre of the injury and significantly enhanced tissue sparing (Fig. 5b,c).

Next, we evaluated whether hIL-10 treatment preserved the connections between the segments caudal to the lesion and various cranial parts of the CNS. To study proprio- and supraspinal connections of the injured spinal cord, few crystals of the retrograde tracer Fast Blue (FB) were placed caudally to the injury into the right L3 segment and the retrogradely labelled neuronal somata in the spinal cord, brainstem and somatomotor cortex were mapped (Fig. 5d,e). Significantly higher numbers of FB-labelled supraspinal (brainstem and motor cortex) and propriospinal (Th5, Th1, C6, and C2 spinal segments) neurons were found in the animals treated with hIL-10 (both *mRNA-hIL-10* and *osm-hIL-10* groups) than in their controls (*SCI* and *mRNA-GFP* groups; Fig. 5f-h). The number of retrogradely labelled neurons in C2 and C6 spinal segments of the mRNA-hIL-10 treated animals was somewhat higher than in the osm-hIL-10 group but this difference did not achieve statistical significance.

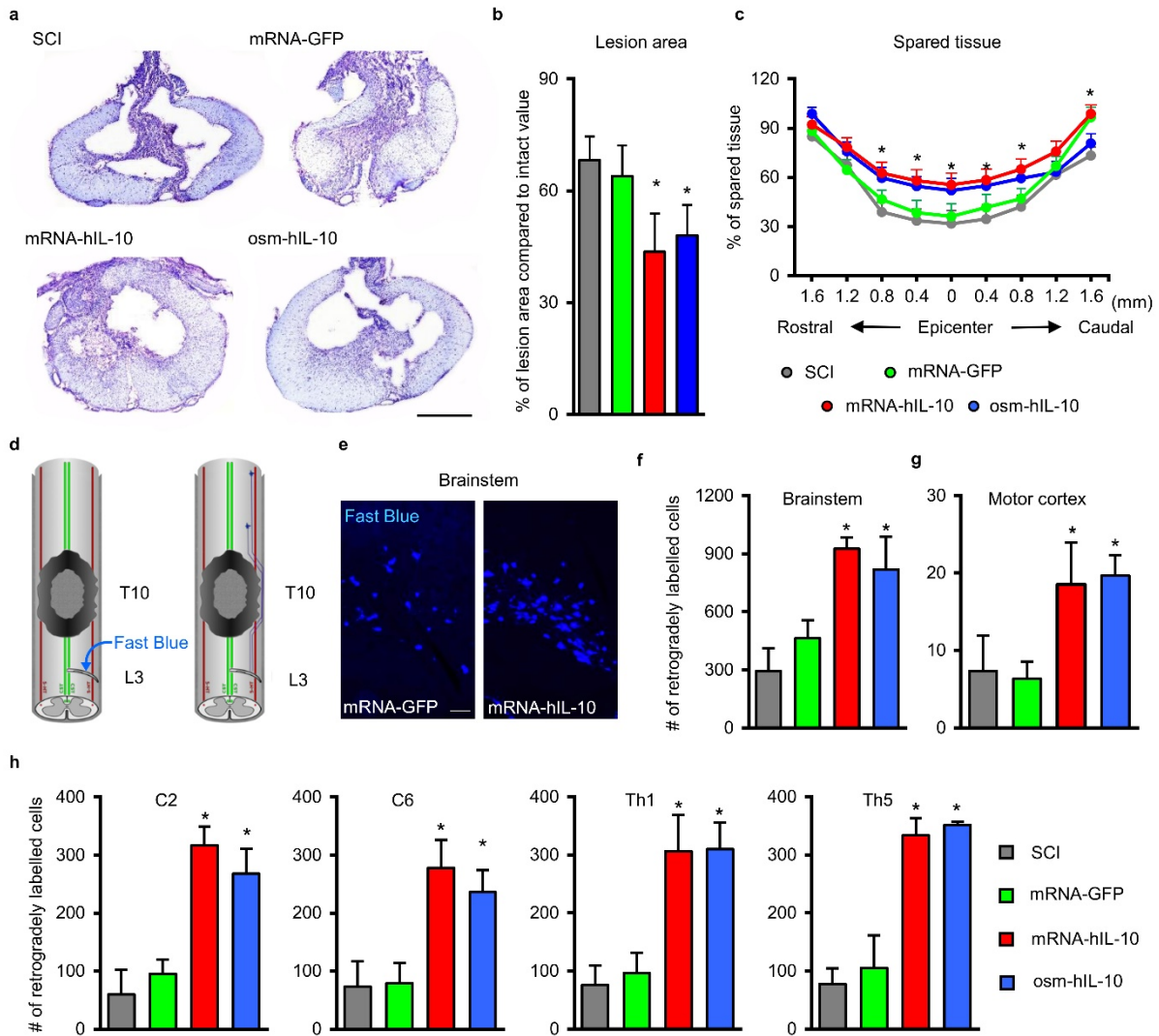


Figure 5. Delayed intraspinal administration of mRNA-LNP encoding hIL-10 induces tissue sparing. **a)** Representative images of cresyl-violet stained sections taken at 100 μ m rostrally from the lesion epicentre. **b)** Quantification of lesion area shows that hIL-10 treatment resulted in significantly reduced size of injury following SCI. **c)** Improved tissue sparing can be seen rostral and caudal to lesion epicentre in hIL-10 treated groups (mRNA-hIL-10 and osm-hIL-10) compared with SCI and mRNA-GFP control animals. **d)** Schematic image shows the retrograde labelling procedure. Fast Blue crystals were placed into the right hemisection gap of the L3 spinal segment. **e)** Retrogradely labelled neurons are shown in the brainstem of mRNA-GFP and mRNA-IL10 animals. **f-h)** Quantification of retrogradely labelled neurons in the brainstem (**f**), in the motor cortex (**g**) and in various spinal segments rostrally from the contusion

injury (**h**). Data represent the mean \pm S.E.M. **a, b, c, f, g** and **h**) $n=4$, biologically independent experiments. $*p < 0.05$ and indicates significant difference between SCI, mRNA-GFP vs. mRNA-hIL-10 and osm-hIL-10 groups. Data were analysed using one-way ANOVA with LSD multiple comparisons test (**a, b, c, f, g** and **h**). Scale bar in **a**=500 μm and in **e**=100 μm .

2.6. mRNA-LNP-induced hIL-10 treatment decreases the microglia/macrophage reaction and modulates cytokine expression in the injured spinal cord.

It is well known that IL-10 is able to suppress inflammatory cytokine expression and the activation of inflammatory macrophages in injured spinal cord (20). In the next series of experiments, we investigated whether the intralesional administration of hIL-10 mRNA-LNP alters the morphological and thus the molecular microenvironment of the lesion area. First, we examined and quantified the GSA-B4-positive microglia/macrophage densities 1, 2 and 5 days after injection in the affected spinal segment. Strong GSA-B4 densities were detected in SCI animals, whose spinal cord displayed high GSA-B4 expression in the epicentre of lesion with considerably weaker staining intensities detected rostrally and caudally from the lesion cavity. Similar expression of CD68 and Iba-1 was observed (Supplement. Fig. 8a-c and Supplement. Fig. 9a-c) Similar changes were found in the animals receiving eGFP mRNA-LNP at all examined time points (Fig. 6a-b). In contrast, moderately decreased GSA-B4 densities were observed following intralesional delivery of hIL-10 mRNA-LNP (Fig. 6c). The quantitative analysis of CD68, Iba-1 and GSA-B4 densities clearly showed that intralesional administration of hIL-10 mRNA-LNP significantly decreased the densities of CD68, Iba-1 and GSA-B4-positive cells compared with the injured spinal cords of *SCI* and *mRNA-GFP* animals at all examined time points (Fig. 6d-f, Supplement. Fig. 8d-f and Supplement. Fig. 9d-f). The significantly suppressed level of microglia/macrophage densities found in the *mRNA-hIL-10* group moved us to hypothesize that there could be a differential production of cytokines in the control (*SCI* and *mRNA-GFP* groups) and treated (*mRNA-hIL-10* group) spinal cords. We evaluated semi-quantitatively the expression of 29 cytokines through the use of the Proteome Profiler array and determined the expression in pooled samples (Fig. 6g-j). On day 5 after hIL-10-LNP treatment, remarkably higher chemiluminescence signal of TIMP-1 and CNTF was measured in the affected segment of the *mRNA-hIL-10* group compared with the *SCI* and the

mRNA-GFP animals. Although protein expression of hIL-10 was significantly decreased 5 days after intraspinal administration of hIL-10 mRNA (Fig. 3c), slightly increased expression of TIMP-1 and CNTF appeared as a time-delayed secondary effect. The circulating cytokines were also evaluated within the first 5 days in blood serum following intralesional injection of saline (*SCI* animals) or mRNA-LNP (*mRNA-GFP* and *mRNA-hIL-10* groups) into the injured cords. No considerable change of cytokine levels was observed in the blood serum of the *mRNA-hIL-10* animals compared with that of the *SCI* or *mRNA-GFP* animals (Supplement. Fig. 10), except for the mild decrease of serum RANTES levels in the *mRNA-hIL-10* group compared with the *SCI* and the *mRNA-GFP* animals by day 5 after treatment. In contrast, CINC-1 serum levels were mildly depressed in *mRNA-hIL-10* and *mRNA-GFP* animals on day 2 compared with the *SCI* animals. These results suggest that intralesional administration of mRNA-LNP encoding hIL-10 has strong anti-inflammatory effect and results in a delayed expression of potent neuromodulatory factors in the affected spinal segments (21). Rat cytokine changes 1 and 2 days after mRNA-LNP administration were detected by PCR analysis (Fig.6k-l). Quantification of IL-6 mRNA in the spinal cord showed significantly increased levels, while that of TNF- α and CCL3 mRNAs revealed significantly decreased levels of these cytokines at both examined time points in the hIL-10 mRNA-treated group (*mRNA-hIL-10*) compared with the *mRNA-GFP* group. IL1- β mRNA levels were significantly decreased on day 1, but showed non-significant changes on day 2 after treatment in the hIL-10 mRNA-treated animals.

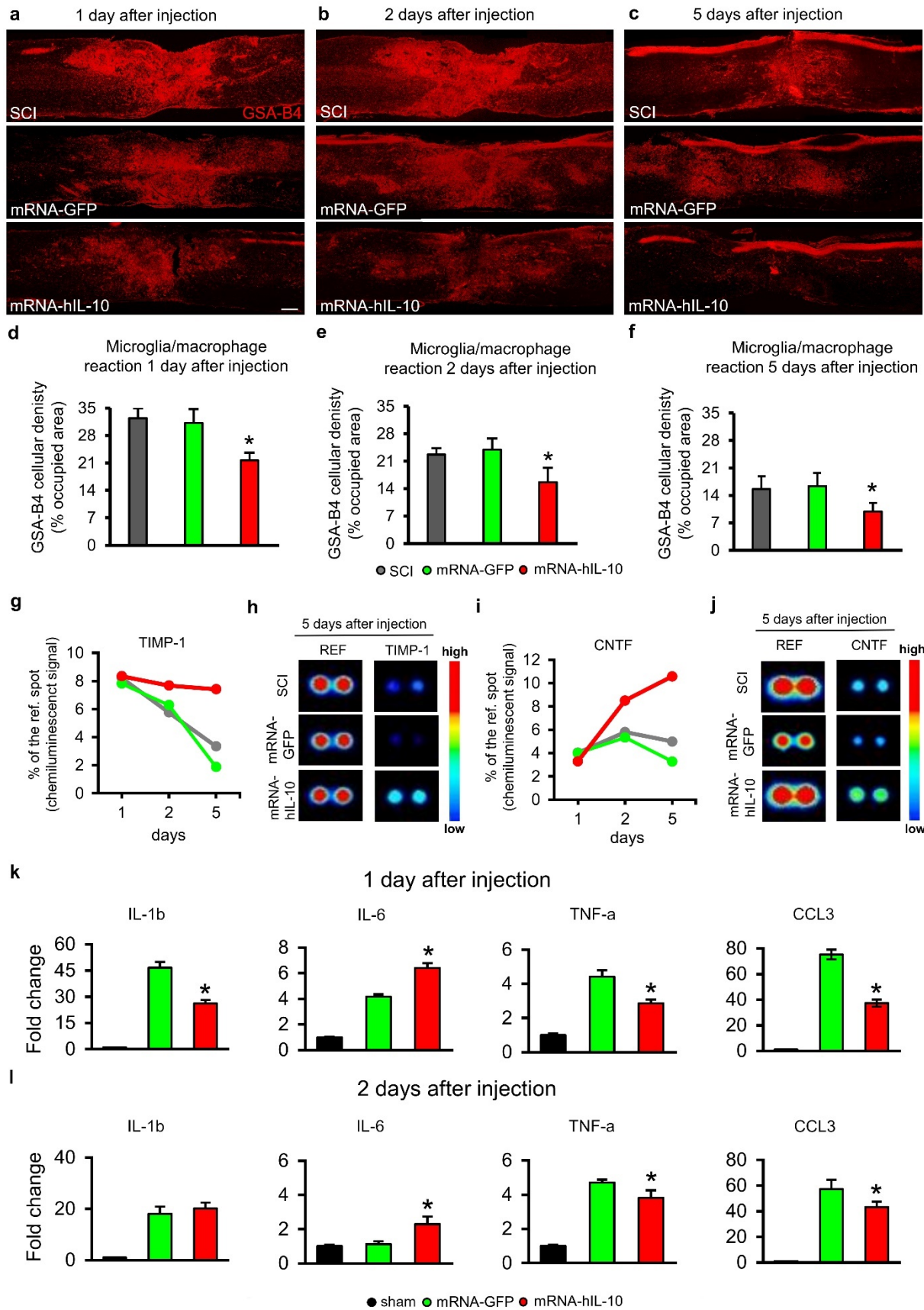


Figure 6. Microglia/macrophage and cytokine changes after mRNA LNP encoding hIL-10 treatment in the injured spinal cord. a-c) Representative images of paramedian sagittal spinal cord sections show the GSA-B4 reactivity 1, 2 and 5 days after intralesional delivery of saline (a), mRNA-LNP encoding eGFP (b) and mRNA-LNP encoding hIL-10 (c) in the lesion area. **d-f)** Quantification of microglia/macrophage (GSA-B4) density in the sagittal sections of the spinal cord revealed significantly decreased level of GSA-B4 at all examined time points in the hIL-10 mRNA treated group (mRNA-hIL-10) compared with the SCI and mRNA-GFP groups. **g-j)** Rodent cytokine level changes were assessed by using the Proteome Profiler array (ARY008) in the spinal cords of SCI, mRNA-GFP and mRNA-hIL-10 groups, comparing the relative levels of 29 rat cytokines. The chemiluminescence signal of spots were compared with reference spots and expressed as % of those. Higher chemiluminescence signals of TIMP-1 (g) and CNTF (i) were detected in the mRNA-hIL-10 group compared with the SCI and mRNA-GFP groups 2 and 5 days after the mRNA-LNP treatment. h) and j) show representative images of REF, TIMP-1 and CNTF spots 5 days after the saline or mRNA-LNP injection. **k-l)** Rat cytokine changes 1 and 2 days after mRNA-LNP administration detected by PCR analysis. Quantification of IL-6 mRNA in the spinal cord showed significantly increased levels, while that of TNF- α and CCL3 mRNAs revealed significantly decreased levels at both examined time points in the hIL-10 mRNA-treated group (*mRNA-hIL-10*) compared with the *mRNA-GFP* group. IL1- β mRNA levels were significantly decreased on day 1, but showed non-significant changes on day 2 after treatment in the hIL-10 mRNA-treated animals. Data were analysed by using one-way ANOVA with LSD multiple comparisons test. Data represent the mean \pm S.E.M. d, e and f: n=4; k-l: n=3 each group, biologically independent experiments. d, e and f: * $p < 0.05$ indicates significant difference between SCI, mRNA-GFP vs. mRNA-hIL-10. k-l: * indicates statistically significant difference ($p < 0.05$) between *mRNA-GFP* vs. *mRNA-hIL-10* groups.

Abbreviations: REF, reference control; TIMP1, Tissue inhibitor of matrix metalloproteinase 1;
CNTF, Ciliary neurotrophic factor; Scale bar in **a**=200 μm .

3. Discussion

Functional and morphological recovery in the injured spinal cord is limited as the considerable primary physical cell death is followed by the development of an unfavourable microenvironment around the damaged neurons. Thus neurons, which are not destroyed by the primary physical damage in the injured cord fail to recover and re-establish their primary connections. In our study, we used nucleoside-modified mRNA to provide a new delivery approach resulting in the expression of the therapeutic protein IL-10 in the injured spinal cord, thus leading to improved neuroprotection and functional outcome.

Nucleoside-modified mRNA-LNP COVID-19 vaccines proved to be safe and effective in humans, opening the way for new applications of the platform such as protein replacement therapy and gene editing (22, 23). Here, we provide evidence that this revolutionary platform can potentially be utilized to successfully treat spinal cord injury and thus to restore motor function. In this work, the expression kinetics of the eGFP mRNA-LNP provided evidence for active translation of mRNA in intact and injured spinal cords. A single injection of a low dose of eGFP mRNA-LNP into intact and injured rat spinal cords resulted in a 3-week-long translation by spinal cord astrocytes. In contrast, neurons in the injured cords expressed GFP for 14 days, whereas eGFP expression in intact spinal cord neurons was limited to a 5 day-long period. It can be argued that the injury itself may have adjusted the cellular metabolic machinery leading to longer eGFP protein expression in the injured neurons. Interestingly, microglia/macrophages were positive for eGFP only for short time, however, astrocytes were able to express eGFP up to 21 days after intraspinal delivery of mRNA-LNP.

Based on the above results mRNA-LNP encoding hIL-10 was administrated intraspinally at the same dose 1 week after the injury. hIL-10 is known to possess a marked anti-inflammatory effect and impart neuroprotection (5, 6, 24). Indeed, we could prove hIL-10 protein production

in neurons and astrocytes for at least 5 days after delivery while microglia/macrophages were found to express hIL-10 for 2 days only. The expression of hIL-10 in astrocytes and neurons indicates that these cell types were primarily targeted by the hIL-10 mRNA-LNP and thus suitable for protein expression. Although the same dose was injected from both eGFP and hIL-10 mRNAs, hIL-10 protein was expressed for a shorter time.

hIL-10 mRNA treatment proved to be effective at inducing significant morphological and functional recovery of the injured spinal cord tissue in rats. Moreover, the functional improvement was non-significantly greater in animals that received hIL-10 mRNA-LNPs compared to rats treated with hIL-10 protein delivered by an osmotic pump to the site of injury (Fig. 4 and 5). These data concord with findings of other laboratories on hIL-10 treatment of injured spinal cord. Park et al. (2018) (6) reported improved functional recovery after spinal cord injury in mice via virus-based IL-10 protein expression, while in another model IL-10 treatment resulted in appearance of vast majority of anti-inflammatory type M2 macrophages in injured spinal cord (5, 25). These findings are in accordance with our results showing that tissue densities of both CD68⁺ macrophages and Iba-1⁺ microglia are downregulated by hIL-10 mRNA-LNP treatment, suggesting a strong anti-inflammatory action of hIL-10 through favourable modulation of microglia/macrophages activities. Intraspinal delivery of hIL-10 mRNA-LNP provides an excellent therapeutic approach compared with virus-based delivery methods and direct administration of hIL-10 protein through the use of osmotic pumps. mRNA-induced protein expression lacks the possible shortcomings of virus-based delivery methods and the relatively invasive nature of the implantation microsurgery of osmotic pumps (9). In our view, delivery of IL-10 via osmotic pumps and the small diameter tubing inserted into the cavity maintained a very minor, but constant damage to the spinal cord until the pump and tubing were removed. This might have led to the minimally depressed functional improvement as compared with the intralesional delivery of hIL-10 mRNA-LNP. This fact further proves that

a relatively short-term, but continuous expression of IL-10 based upon mRNA delivery is at least as effective as treatment with recombinant IL-10.

Interestingly, significant, but short-term hIL-10 protein expression was detected in serum only on the first day after the intraspinal administration of hIL-10 mRNA-LNP, possibly due to the fact that spinal cord contusion injury leaves the blood-brain-barrier open for weeks if not months (26). Moreover, intraspinal administration of hIL-10 mRNA-LNP is a secondary intervention after injury inducing some bleeding and macrophage/lymphocyte migration. It is also conceivable that IL-10 will also be expressed for a short time by cells entering and leaving the injured spinal cord. The very limited production of hIL-10 in the serum indicates that intraspinal mRNA delivery is a minimally invasive route of administration in experimental animals and this procedure can likely be further improved. Proteome Profiler array investigation of the serum circulating cytokine profile resulted in only one considerable change at short-term. CINC-1 showed a mild systemic decrease 2 days after administration of hIL-10 and eGFP mRNA-LNP, while the pro-inflammatory RANTES serum level also mildly dropped in mRNA-hIL-10 animals 5 days after hIL-10 treatment. CINC-1 is expressed by number of cells such as macrophages, neutrophils, and epithelial cells and contributes to angiogenesis, inflammation and wound healing (27, 28). It is thought that the mild systemic changes of these cytokines occurring few days after intraspinal hIL-10 administration are not likely to influence the repair and regenerative mechanisms in the spinal cord.

We were interested what cellular and molecular changes were induced by the hIL-10 mRNA - LNP treatment in the injured rat spinal cord. Delayed intraspinal administration of hIL-10 mRNA-LNP resulted in decreased microglial activity within the first 5 days after delivery and showed a time-delayed secondary effect with increased TIMP-1 and CNTF levels compared with the control animals. It has been shown that increased levels of circulating TIMP-1 after

brain injury may contribute to the preservation of the blood-brain barrier and mediate cytoprotection via the regulation of microglial activity (29-31). CNTF is a neurotrophic factor that promotes remyelination by grafted or endogenous oligodendrocyte precursor cells after spinal cord injury and decreases myelin loss as well as the severity of functional loss after experimental autoimmune encephalomyelitis (32, 33). PCR-based quantification of IL-6 mRNA in the spinal cord showed significantly increased levels, while TNF- α and CCL3 mRNAs decreased significantly at both examined time points in the hIL-10 mRNA-treated animals (*mRNA-hIL-10*) compared with the data of the *mRNA-GFP* group. IL-1 β mRNA levels proved to be significantly decreased only on day 1 in the hIL-10 mRNA-treated animals. The limited effect of IL-10 treatment on IL-1 β has also been found in other, in vitro experiments, where IL-10 in primary glial cultures (astrocytes, microglia and mixed cell cultures) was unable to influence IL-1 β levels, but downregulates other cytokines, eg. IL-6, TNF- α (21). While the rapid downregulation of the inflammatory cytokines IL-1 β , TNF- α and CCL3 clearly indicates the beneficial effect of hIL-10 therapy, the increase of IL-6 mRNA levels does not seem to fit into the classical view of peripheral immune responses. The increased gene expression of IL-6 can be explained by the recent findings by several, including our publications that, IL-6 may have an anti-inflammatory/immunoregulatory effect in the CNS (9, 34), despite its proinflammatory peripheral role. Taken together, these factors may have actively contributed to the downregulation of microglial activity and the maintenance of the integrity of spinal cord after spinal cord injury.

4. Materials and Methods

4.1. mRNA-LNP production

Codon-optimized enhanced green fluorescent protein (eGFP) and human interleukin 10 (hIL-10) were synthesized and cloned into the mRNA production plasmid as described earlier (35). mRNA production and LNP encapsulation was performed according to our protocols (35). Briefly, mRNAs were transcribed to contain 101 nucleotide-long poly(A) tails. m¹Ψ-5'-triphosphate (TriLink) instead of UTP was used to generate modified nucleoside-containing mRNA. Capping of the *in vitro* transcribed mRNAs was performed co-transcriptionally using the trinucleotide cap1 analog, CleanCap (TriLink). mRNA was purified by cellulose (Sigma-Aldrich) purification (36). All mRNAs were analyzed by agarose gel electrophoresis and were stored frozen at -20°C. Cellulose-purified m¹Ψ-containing RNAs were encapsulated in LNP using a self-assembly process as previously described wherein an ethanolic lipid mixture of ionizable cationic lipid, phosphatidylcholine, cholesterol and polyethylene glycol-lipid was rapidly mixed with an aqueous solution containing mRNA at acidic pH (37). The ionizable cationic lipid (pKa in the range of 6.0-6.5, proprietary to Acuitas Therapeutics) and LNP composition are described in the patent application WO 2017/004143. The mean hydrodynamic diameter of mRNA-LNP was ~80 nm with a polydispersity index of 0.02-0.06 as measured by dynamic light scattering using a Zetasizer Nano ZS (Malvern Instruments Ltd, Malvern, UK) and an encapsulation efficiency of ~95% as determined using a Ribogreen assay mRNA-LNP were stored at -80°C.

4.2. Spinal cord injury model and intraspinal delivery of mRNA-LNP complexes into intact and injured animals

Surgical procedures and animal care were performed according to the Animal Care and Use Committee guideline at the University of Szeged. A rat contusion model of SCI was performed

as described previously (9, 38). Sprague-Dawley female rats (n= 203; 220-240 g body weight, animals were randomly chosen for the various treatment groups, for details see Supplement. Table 1.) were anesthetized using (ketamine hydrochloride [Ketavet, 110 mg/kg body weight]; xylazine [Rompun, 12 mg/kg body weight]) and sterile precautions. After the dorsal laminectomy at the T10 vertebral level, the contusion injury was induced by using a custom-made spinal cord impactor, applying 150 kdyn force. The superficial back muscles and the skin were sutured in layers. For postoperative animal care, saline (0.9%; 5 ml) to prevent dehydration and meloxicam (Metacam; 0.5 mg/kg body weight, Boehringer Ingelheim Vetmedica) were administrated. Their bladders were manually expressed three times a day until reflexive function was observed. At 7 days after the injury, 3.0 µg of mRNA-LNP (eGFP-mRNA or hIL-10-mRNA) in Dulbecco's Phosphate Buffered Saline (PBS) were injected into animals intraspinally (3 µl) into the forming lesion cavity with a Hamilton pipette. Injured control animals (*SCI group*) received only contusion injury.

In intact animals the lamina of T10 vertebra was removed and the dura was opened. mRNA-LNP (3.0 µg) were administrated into the intact spinal segment. Postoperative animal care was performed as described above. Experimental schematic of short- and long-term studies is shown in Supplement Fig. 1.

4.3. Administration of hIL-10 via osmotic pump

One week after the contusion injury, a miniature osmotic pump (Alzet Osmotic Pumps, Cupertino, CA; type 1002, 100 µL volume, actively pumping for 2 weeks,) filled with hIL-10 (4 µg/mL working concentration, from R&D Systems, Minneapolis, MN) was placed subcutaneously in the back region. A silicone tube (Degania Silicone Ltd, Kibbutz Degania, Israel, 0.3 mm in internal diameter) extended from the pump to the spinal cord, and its distal

end was inserted into the contusion cavity (9). The tube was fixed to the surrounding musculature with 8-0 sutures (Ethilon) to avoid moving in or out of the spinal cord (9).

4.4. Histo- and immunohistochemistry

Cross section and longitudinal paramedian sagittal sections (25 and 16 μm thickness) taken from the spinal cord including the lesion site were cut in a cryostat (Leica CM-1860, Leica GmbH, Germany) and mounted onto gelatinized slides. After 20 min air-drying, the sections were permeabilized with 0.5 % Triton X-100 in PBS for 5 minutes and blocked for 1 h at 24°C with 5% BSA in PBS. Primary antibodies and lectin were used overnight at 4°C as follows: chicken anti-GFP (1:1000, ab13970, Abcam), rabbit anti-IL-10 (1:400, ab34843, Abcam), rabbit anti-GFAP (1:500, 7260, Abcam), goat anti-GFAP (1:500, ab53554, Abcam), rabbit anti-TUBB3 (1:500, ab18207, Abcam), mouse anti-TUBB3 (1:500, ab7751, Abcam), goat anti-Iba1 (1:400, ab5076), anti-CD68 (1:200, MAB101141, R&D Systems) and biotinylated Griffonia simplicifolia isolectin B4 (GSA-B4, 1:200, B1205, Vector Laboratories). The following secondary antibodies were used: biotinylated goat anti-rabbit IgG (1:200, BA-1000, Vector Laboratories). The immune reaction was completed by Alexa Fluor 488 goat anti-chicken (1:600, A11039, Thermo Fisher Scientific), Alexa Fluor 488 goat anti-rabbit (1:600, A11008, Thermo Fisher Scientific), Alexa Fluor 488 donkey anti-goat (1:600, A11055, Thermo Fisher Scientific), Alexa Fluor 546 donkey anti-rabbit (1:600, A10040, Thermo Fisher Scientific), Alexa Fluor 594 donkey anti-goat (1:600, A11058, Thermo Fischer Scientific), Alexa Fluor 594 goat anti-mouse (1:600, A21203, Thermo Fisher Scientific) and Streptavidin Alexa Fluor 488 (1:600, S11223, Thermo Fisher Scientific). The sections were covered using Vectashield mounting medium containing DAPI (1.5 $\mu\text{g}/\text{ml}$; H-1000-10, Vector Laboratories), which labelled the nuclei of the cells. Negative controls for the secondary antibodies were performed by omitting the primary antibodies.

Immunoreactive sections were analyzed by using a BX-41 epifluorescent microscope (Olympus Ltd. Tokyo, Japan) equipped with a DP-74 digital camera and its CellSens software (V1.18, Olympus), a Panoramic MIDI II slide scanner (3DHitech Ltd, Budapest, Hungary) equipped with Panoramic Scanner 2.1.2 software (3DHitech) and an Olympus Fv-10i-W compact confocal microscope system (Olympus) with the Fluoview Fv10i software (V2.1, Olympus).

4.5. Quantification of microglia/macrophage density

For quantifying CD68, Iba-1 and GSA-B4 reactivity, analysis was performed according to Arevalo-Martin et al. (39). Four parasagittal sections (150 μ m apart from each other) containing the lesion area were analysed, 8, 9 and 12 days after injury in the SCI, mRNA-GFP and mRNA-hIL-10 groups. Microphotographs were taken using an Olympus BX-41 epifluorescence microscope equipped with a DP-74 digital camera and the whole spinal cord section area including the lesion area and a 2 mm long extension of the tissue rostrally and caudally from the cavity ends was analysed using the ImageJ software (NIH). The background intensity of unstained samples was individually subtracted from the intensity of treated sections. Iba-1, CD68 and GSA-B4 positive areas (size of areas was expressed in pixels) of the injured spinal cords were then divided by the size of examined area and multiplied by 100.

4.6 Quantification of GFAP, TUBB3 and GSA-B4 colocalization with eGFP and hIL-10

Three spinal cords from each group were processed for immune- and histochemistry (eGFP/GFAP, eGFP/TUBB3, eGFP/GSA-B4, hIL-10/GFAP, hIL-10/TUBB3 and hIL-10/GSA-B4). The measurement was performed in 6500 μ m width and 1500 μ m height rectangle shaped frame around the injected area. The evaluation was performed by HistoQuant software (QuantCenter multiple-module image analysis platform; 3DHISTECH). The animals that received eGFP encoding mRNA were investigated at six time points (1 day, 2 days, 5 days, 9 days, 14 days and 21 days) after injection, the hIL-10 mRNA treated rats were only examined

on day 1, 2 and 5 after injection. Data were expressed as percentage of colocalized area of marker / total area of marker ratio.

4.7. Proteome profiler arrays

The rat spinal cord fractions were homogenized in PBS with protease inhibitor (Sigma). After homogenization Triton X-100 (Sigma) was added to a final concentration of 1%. The samples were frozen to -75 °C, thawed and centrifuged at 10,000 x g for 5 minutes. The supernatant was collected and the total protein concentration was determined by using the Pierce BCA Protein Assay Kit (Thermo Scientific). The blood samples were allowed to coagulate for 1 hour at room temperature and then at 4 °C overnight. The sera were collected after centrifugation of the blood at 1000 x g for 5 minutes. The cytokine and chemokine contents of the samples (spinal cord and serum) were determined using the Proteome Profiler Rat Cytokine Array Kit, Panel A (R&D Systems, Minneapolis, MN). For the parallel determination of the relative levels of selected rat cytokines and chemokines, we used 390 µg total protein of spinal cord homogenates and 600 µl serum on each membrane. The spinal cord (130 µg total protein each) samples and sera (200-200 µl each) were pooled from 3 animals/group. The assay was performed following the manufacturer's instructions. The chemiluminescent signals from the bound cytokines present in the spinal cord and sera were detected using the LI-COR Odyssey Imaging System and analysed with Image Studio Software.

4.8. RNA isolation and real-time polymerase chain reaction (qPCR)

In total, 18 rats were used for the PCR analysis. Treated animals were allowed to survive 8 or 9 days after the contusion injury (1 or 2 days after mRNA treatment) in order to study the time-dependent changes in mRNA expression of inflammatory components and mediators in the spinal cord. To assess the effect of mRNA-hIL10 treatment on the expression of genes such as IL1B, IL6, TNFA and CCL3, animals were divided into three groups (sham-operated, mRNA-

GFP control, and mRNA-hIL10 treated). Animals in the sham-operated group were sacrificed one day after surgery.

Animals were transcardially perfused with physiological saline after the appropriate postoperative time, and the Th10 spinal cord segment was dissected. Spinal cord samples were homogenized in TRIzol reagent (Cat.# 15596026, Thermo Fisher Scientific, Waltham, MA, USA) and the total RNA was extracted by using the Direct-zol RNA Miniprep kit (Cat#R2050, Zymo Research, Inc., Irvine, CA, USA). The amount of RNA was determined by using a spectrophotometer (Spectrostar^{Nano}, BMG Labtech, Germany). To transcribe cDNA from RNA, Maxima First Strand cDNA Synthesis Kit was applied (Cat# K1672, Thermo Fisher Scientific). RT-qPCR was carried out using a Bio-Rad CFX96 Real-Time PCR instrument (RRID:SCR_018064; Bio-Rad, Hercules, CA, USA) and Luminaris Color HiGreen qPCR Master Mix, fluorescein (Cat# K0381, Thermo Fisher Scientific, Waltham, MA, USA) under the following parameters: 40X (95 °C/15 s, 60 °C/30 s and 72 °C/30 s). Primer sequences for each gene were as follows: **IL1B** Fw: TGGCAACTGTCCCTGAACTC, Rev: AAGGGCTTGGAAGCAATCCTT, **IL6** Fw: TCCGGAGAGGAGACTTCACA, Rev: GAATTGCCATTGCACAACCTT, **TNFA** Fw: GATCGGTCCCAACAAGGAGG, Rev: CTTGGTGGTTTGCTACGACG, **CCL3** Fw: GCTTCTCCTATGGACGGCA, Rev: CTCTTGGTCAGGAAAATGACACC. Gene expression data were normalized to GAPDH.

4.9. Human interleukin-10 enzyme-linked immunosorbent assay

The human IL-10 content of the rat samples was evaluated by using a human IL-10 ELISA Kit (Sigma-Aldrich). The spinal cord samples were diluted to 2 mg/ml total protein concentration; the sera were diluted two-fold and the samples were tested in duplicate. The experiment was performed following the factory's sandwich ELISA instructions.

Briefly, the diluted rat spinal cord and sera samples were run in 100 μ l. After 2.5 hours incubation at room temperature the plate was washed and covered with detection antibody for one hour. The washing step was repeated, after which the Streptavidin Solution was added for 45 minutes. After washing the wells with 300 μ l Wash Buffer 4 times, the TMB Substrate Solution was added, then, after 30 minutes incubation the reaction was stopped by adding the Stop Solution. The absorbance was measured at 450 nm.

4.10. Retrograde labelling and quantitative assessment of retrogradely labelled neurons

Retrograde labelling was performed as described previously (9, 38). Briefly, the L2-4 spinal segments were explored 9 weeks after the injury. At the level of L3 spinal segment a right hemisection was performed. Fast Blue (FB) crystals (0.5 mg in each case, Chemimart GmbH, Berlin, Germany) were gently placed into the hemisection gap and the wound was closed. Seven days after the application, the animals were re-anesthetized and perfused transcardially. Transversal sections (30 μ m thick) taken from the motor cortex, brainstem and spinal cord (C2, C6, T1 and T5 spinal segments) were cut in a cryostat (Leica CM-1860, Leica GmbH, Germany) and mounted onto gelatinized slides. Every transverse section from the T5, T1, C6 and C2 spinal segments and every 5th or 10th coronal section from the brainstem or the brain were used, respectively.

4.11. Morphometric analysis of the lesion area and spared tissue

Every fourth transverse section from the T8-L1 segments containing the lesion cavity was stained with cresyl-violet (1% aqueous cresyl-violet solution, C-1791, Sigma-Aldrich) (n = 4 in each group). The border between the intact tissue and the lesion cavity composed of small cysts was defined. The whole cystic cross-sectional area (lesion cavity area) at the level of the epicentre was determined as follows: the number of pixels of the reference area (1 mm²) and that of the cystic area was computed through the use of the NIH ImageJ analysis software

(imagej.nih.gov/ij). The pixel number of the cystic area was divided by that of the reference area and the result was expressed in percentage of lesion area compared to intact value.

The number of pixels of the spared tissue was measured at the epicentre (0) and 0.4, 0.8, 1.2, and 1.6 mm rostrally and caudally from it. Identical spinal cord segments of intact animals were used as reference values. The amount of spared tissue in the long-term groups was given as percentage of intact spinal cord values.

4.12. Open field test for locomotor recovery

To test the motor function recovery in the long term survival groups (9 weeks), BBB test was used at three days after the injury and once a week for 9 weeks (18). Two observers evaluated the hindlimb locomotor function of animals in an open field (150 × 100 cm) for 4 min at a similar time of day for each testing.

4.13. Video-based motor functional analysis

On the 9th postoperative week, a multi-parametric kinematic analysis was carried out with a custom-made system developed in our laboratory (19, 38). The method allows the measurement of different joint angles in different moments of the step cycle. To achieve this, two high speed cameras (one from lateral and one from rear aspect) and a mirror system were implemented surrounding a runway where the animals could walk into only one direction. The knee flexion, the ankle flexion, the knee lifting and the ankle lifting parameters were recorded from lateral aspect together with the metatarsus-surface angle (MSA) and tibia-surface angle (TSA) observed from rear-view. We chose these parameters as our earlier studies proved these to be appropriately efficient in this phase of the motor recovery (19, 38).

4.14. Statistical analysis

Student's t-test was used to compare two groups and one-way ANOVA with LSD post-hoc test to compare more than two groups. BBB scores was analysed using repeated measures ANOVA

with LSD post-hoc test. The level of significance was set at $p < 0.05$, and all error bars represent the standard error of mean (SEM).

Acknowledgement

Author Contributions: A.N., K.P. and L.G. designed the experiments. L.G., T.B., K.P., Z.F., D.T. performed the surgical and gait analysis experiments. L.G. and R. B. collected the samples and managed all tissue processing, staining and imaging. A.M. and C.V. performed and analysed the proteome profiler and ELISA. M.B.B. and P.J.C.L. prepared the LNPs. R.K. performed the PCR experiments and data analysis. L.G., T.B., K.P., Z.F. prepared the figures. A.N., K.P. and N.P. wrote the manuscript. N.P., D.W., M.B.B., P.J.C.L. and A.N. revised the manuscript. All authors discussed and helped prepare the manuscript. We thank Sudheer Babu Sangeetham for the professional assistance (Department of Anatomy, Histology and Embryology, Szent-Györgyi Albert Medical School, University of Szeged).

Funding: N.P. was supported by NIH R01-AI153064. C.V and A.M. received generous support from the following grants: 2020-1.1.6-JÖVŐ-2021-00012 and 2022-2.1.1-NL-2022-00008 for the National Biotechnology Laboratory. A.N. was supported by the NKFIH KLINO-117031 grant.

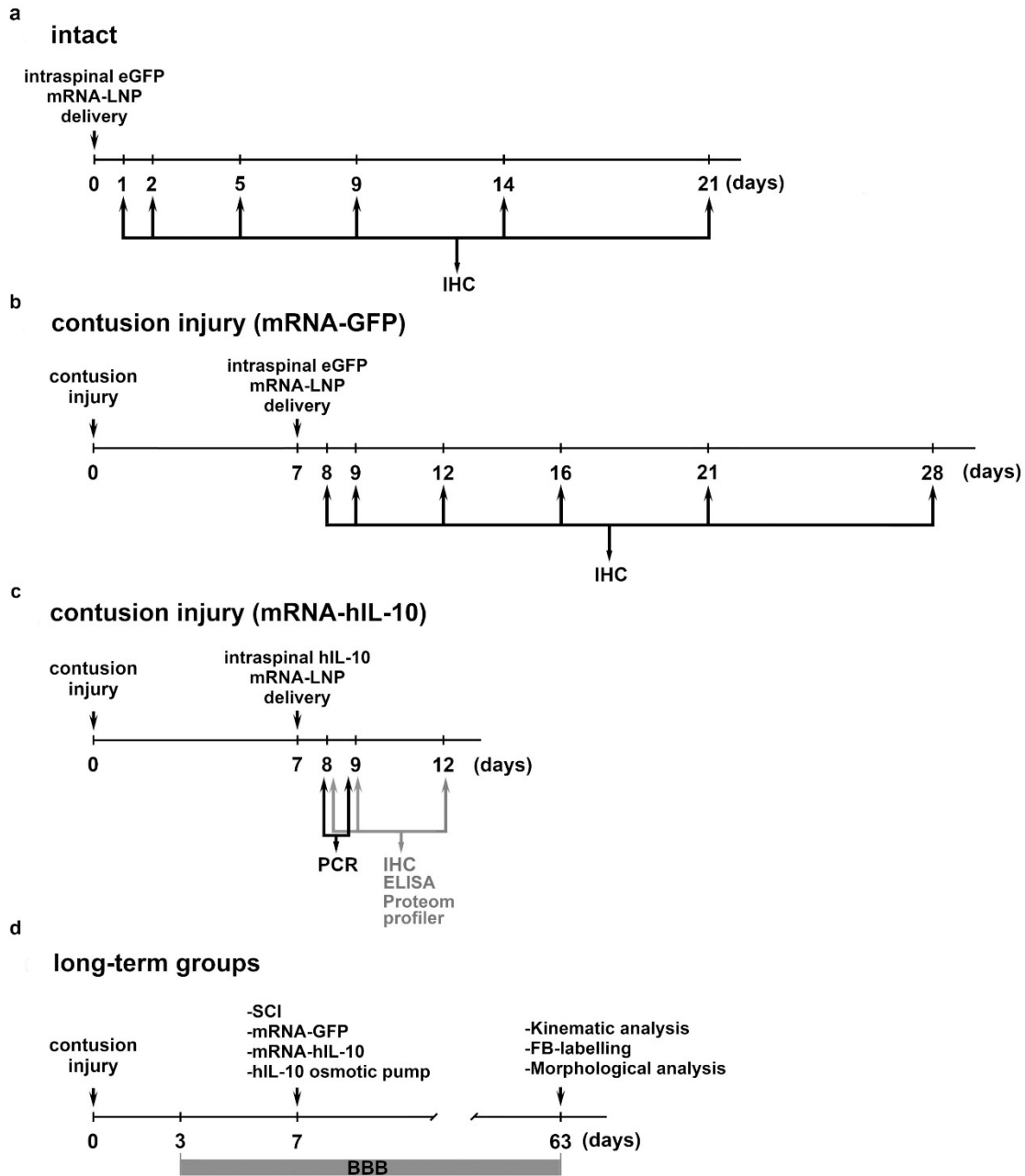
Conflict of Interest: The authors declare that there is no conflict of interest regarding the publication of this article.

Data Availability: All data needed to evaluate the conclusions in the paper are present in the paper and/or the Supplementary Materials.

Supplementary Materials

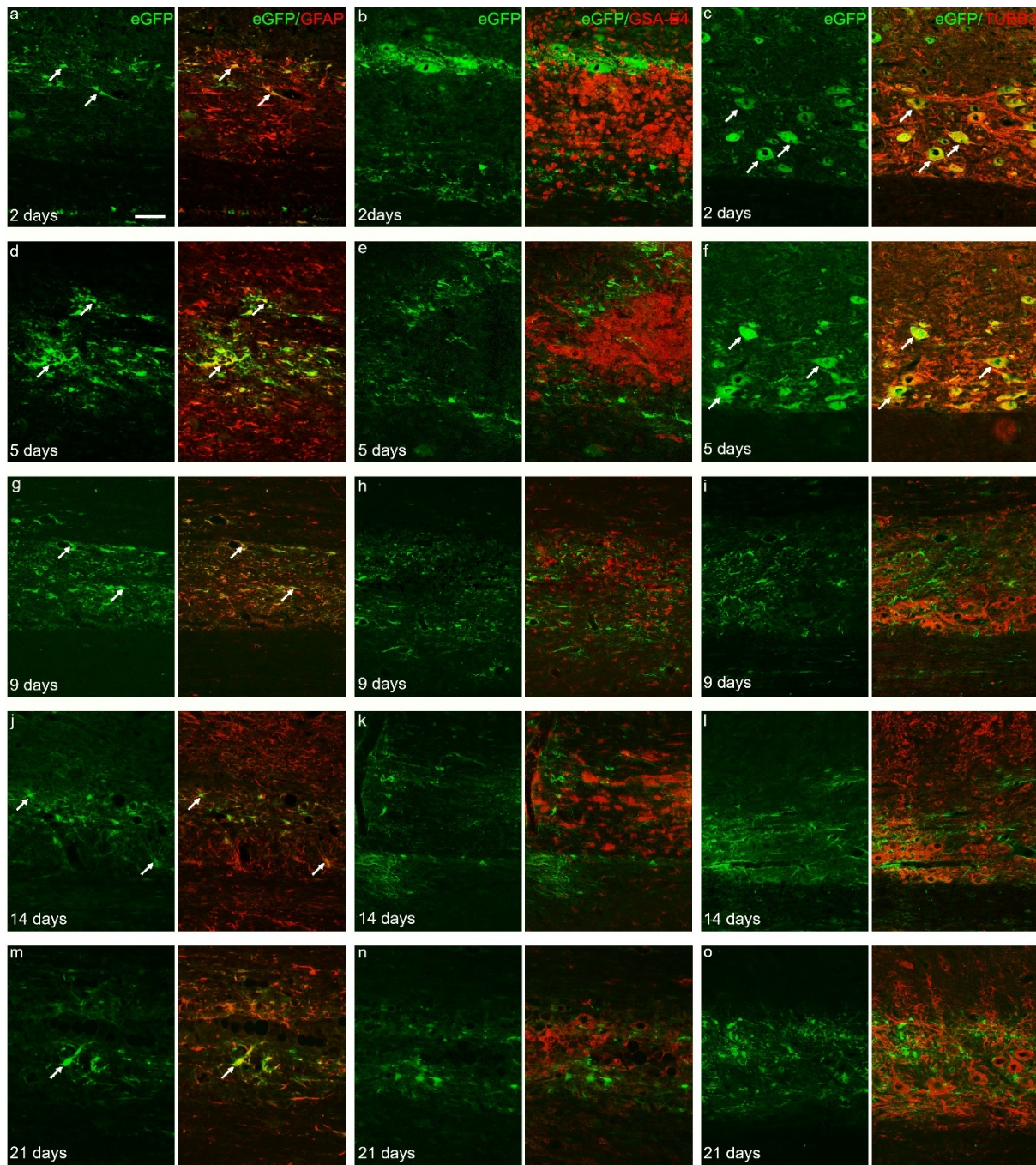
Supplementary Table 1. The table provides information on the number of animals used for the various experimental setups and purposes.

Exp. groups Procedures	Intact	SCI	mRNA- GFP	mRNA- hIL-10	osm- hIL-10	sham
immunohistochemistry for short term study	18	18	36	9	-	-
ELISA	-	12	12	12	-	-
Proteome profiler	-	12	12	12	-	-
PCR	-	-	6	6	-	6
morphological analysis, Fast Blue labelling and functional tests for long term study	-	8	8	8	8	-

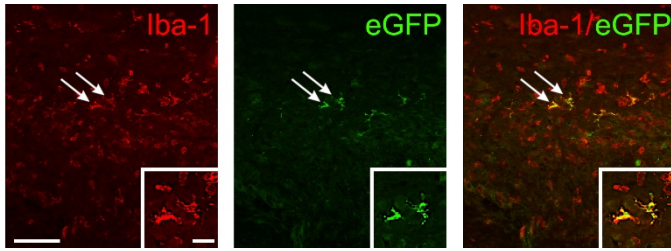


Supplementary Figure 1. Illustration depicting the short- and long-term experiments and the protocols applied. Intact adult female rats (220 to 250 g) underwent contusion injury at the T10 vertebral level. On day 7 after the injury, a single dose of mRNA-LNP (3.0 μ g) or saline was administered in to the injured rat spinal cord. **a-c)** In the short-term study at 1, 2, 5, 9, 14 and 21 days after the injection, the spinal cords were collected from the intact (**a**) and injured rats (**b**) that received saline or mRNA-LNP encoding eGFP. Immunohistochemistry (IHC) was

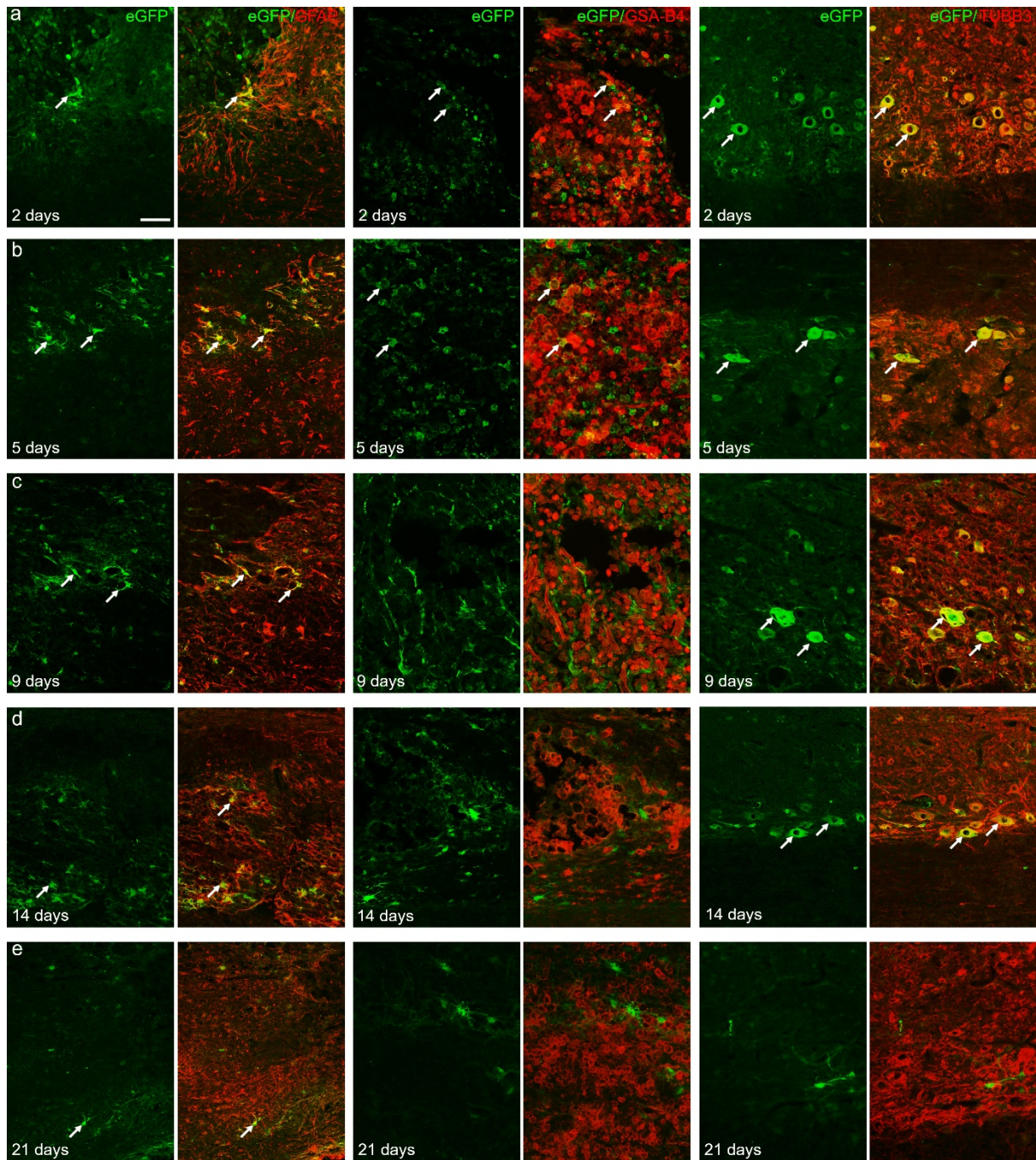
performed to study the eGFP expression at various time points. **c)** Another group of rats were treated with mRNA-LNP-encoding hIL-10 1 week after the injury. The hIL-10 expression was analyzed 1, 2, 5 and 9 days after mRNA-LNP treatment. Other rats were used for various assays to analyze the acute inflammatory response and hIL-10 expression. **d)** In the long-term study, open field locomotor test (BBB) was applied on day 3 after SCI, followed by weekly assessments up to 9 weeks in the following groups (SCI, mRNA-GFP, mRNA-hIL-10 and osm-hIL-10 group). Gait parameters were determined through the use of a plexiglass runway equipped with a mirror system and cameras recording both lateral and rear-view aspects. Retrograde labelling from the L3 spinal segment and morphological analysis were performed to identify the number the retrogradely labelled neurons rostral to the injury and quantify the tissue preservation at the lesion site, respectively.



Supplementary Figure 2. eGFP expression in the intact rat spinal cord. a-c) Rat astrocytes and neurons but not GSA-B4 cells show strong eGFP expression at 2 days post-injection. **d-f)** Similar eGFP expression can be seen 5 days after delivery of mRNA-LNP. **g-i)** Nine days after mRNA-LNP administration only astrocytes express eGFP. **j-o)** Astrocytes expressed eGFP up to 21 days after intraspinal mRNA-LNP administration. Arrows show co-localizing cells. Scale bar in **a**=50 μ m.

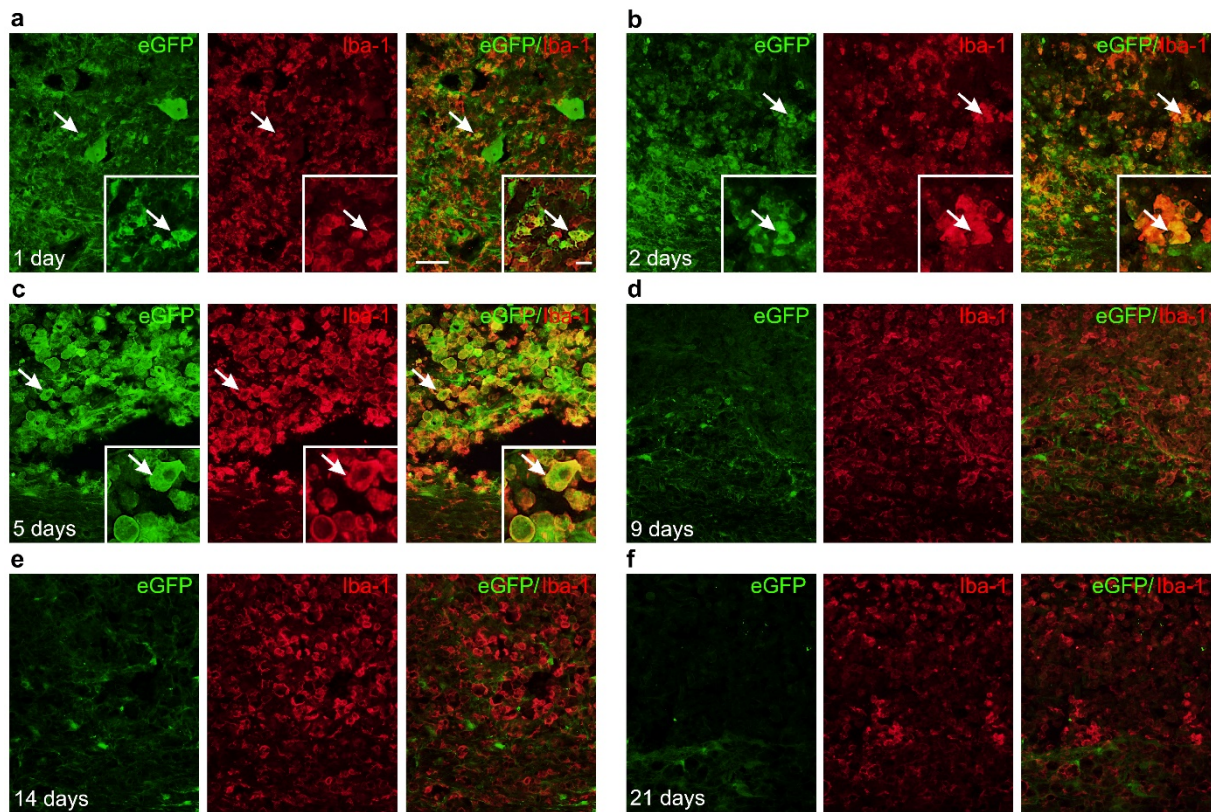


Supplementary Figure 3. eGFP expression in Iba-1 positive cells in intact spinal cord. Representative images show Iba-1-positive cells co-localized with eGFP in the intact spinal cord 1 day after intraspinal delivery of mRNA-LNP encoding eGFP. Arrows indicate the co-localized cells. Scale bar: 100 μ m and 20 μ m

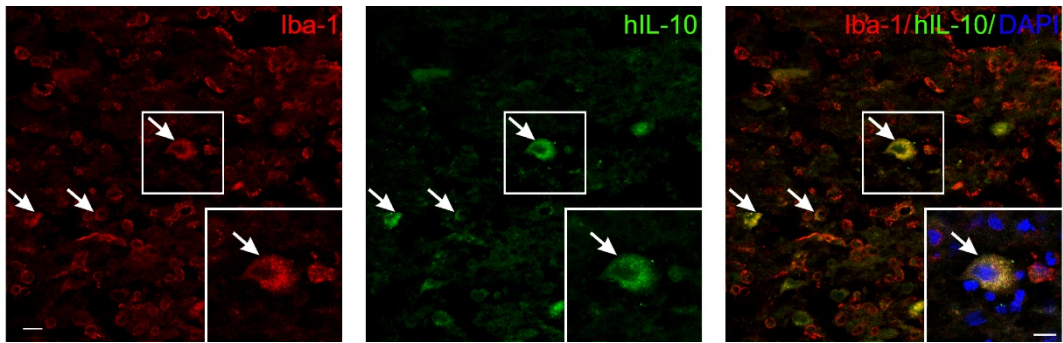


Supplementary Figure 4. eGFP expression in the injured rat spinal cord. a, b) Astrocytes, (GFAP), microglia/macrophages (GSA-B4) and neurons (TUBB3) displayed strong eGFP expression 2 and 5 days after mRNA-LNP delivery in or around the lesion area. **c, d)** Images demonstrate the presence of eGFP in astrocytes and neurons, but not in GSA-B4-positive cells 9 and 14 days after mRNA-LNP delivery. **e)** On day 21 after intraspinal mRNA-LNP treatment

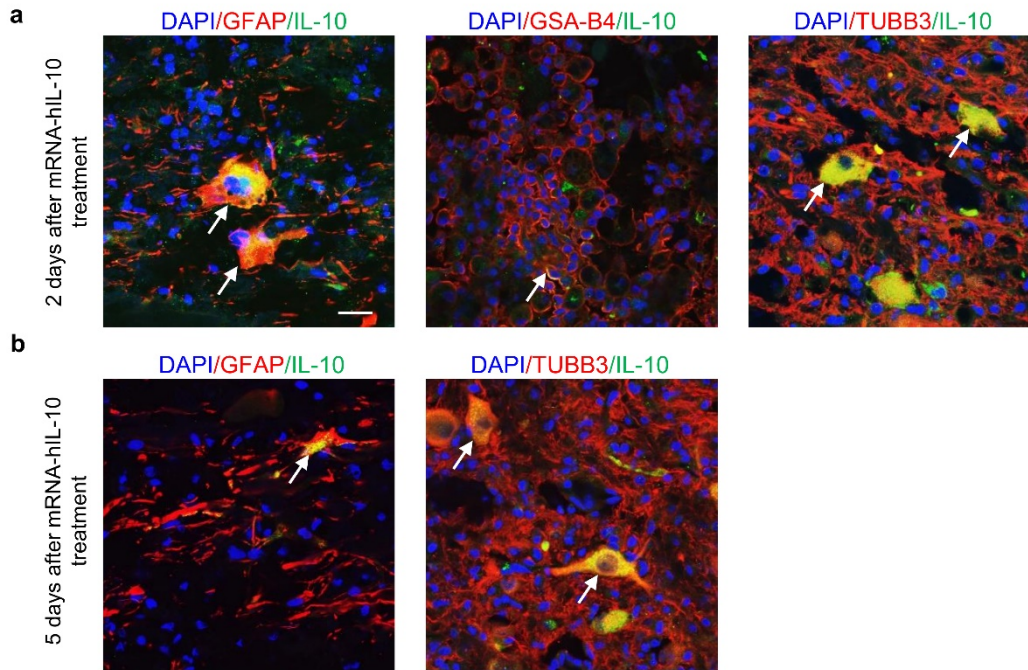
only astrocytes co-localized GFAP with eGFP. Arrows show co-localizing cells. Scale bar in **a**=50 μm .



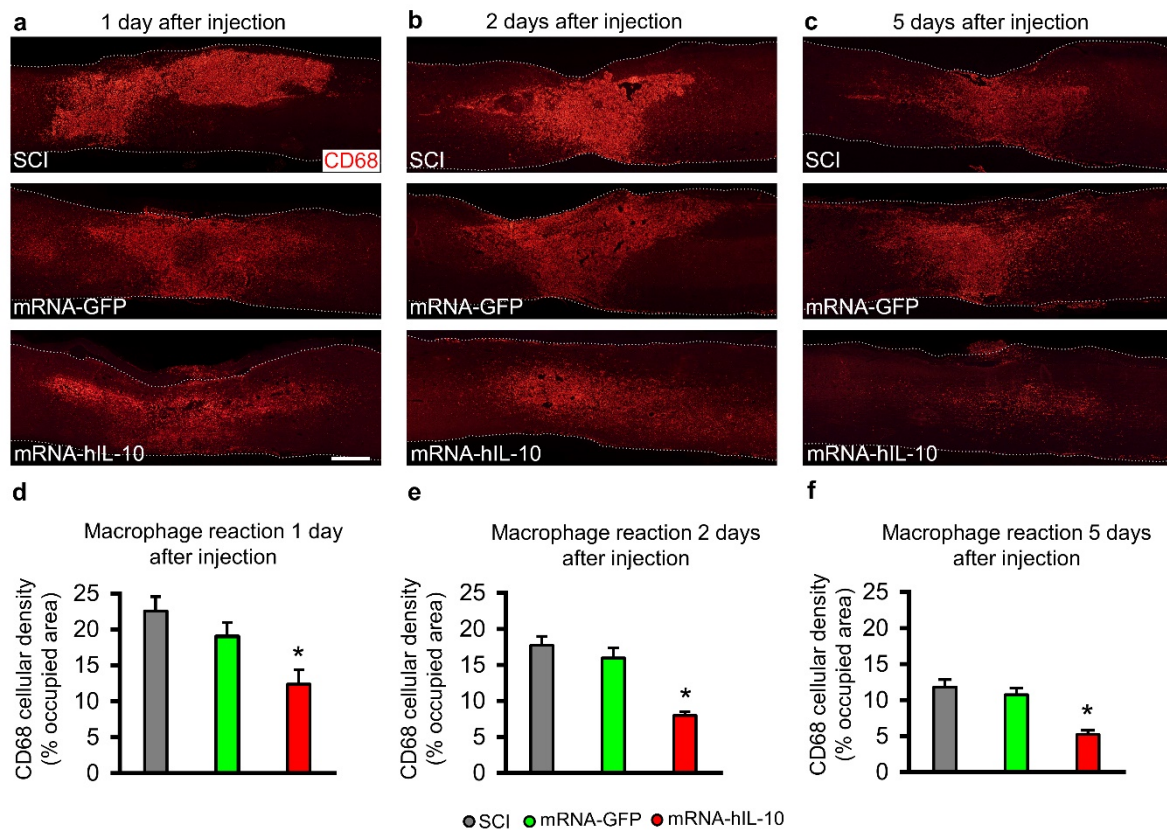
Supplementary Figure 5. eGFP expression in Iba-1-positive cells in the injured rat spinal cord. a-c) Images demonstrate the presence of eGFP in Iba-1-positive cells 1, 2 and 5 days after mRNA-LNP delivery in or around the lesion area. **d-f)** On days 9, 14 and 21 after intraspinal mRNA-LNP treatment no eGFP-positive microglia cells were detected. Arrows show co-localized cells. Scale bar in **a**=50 μ m and 20 μ m.



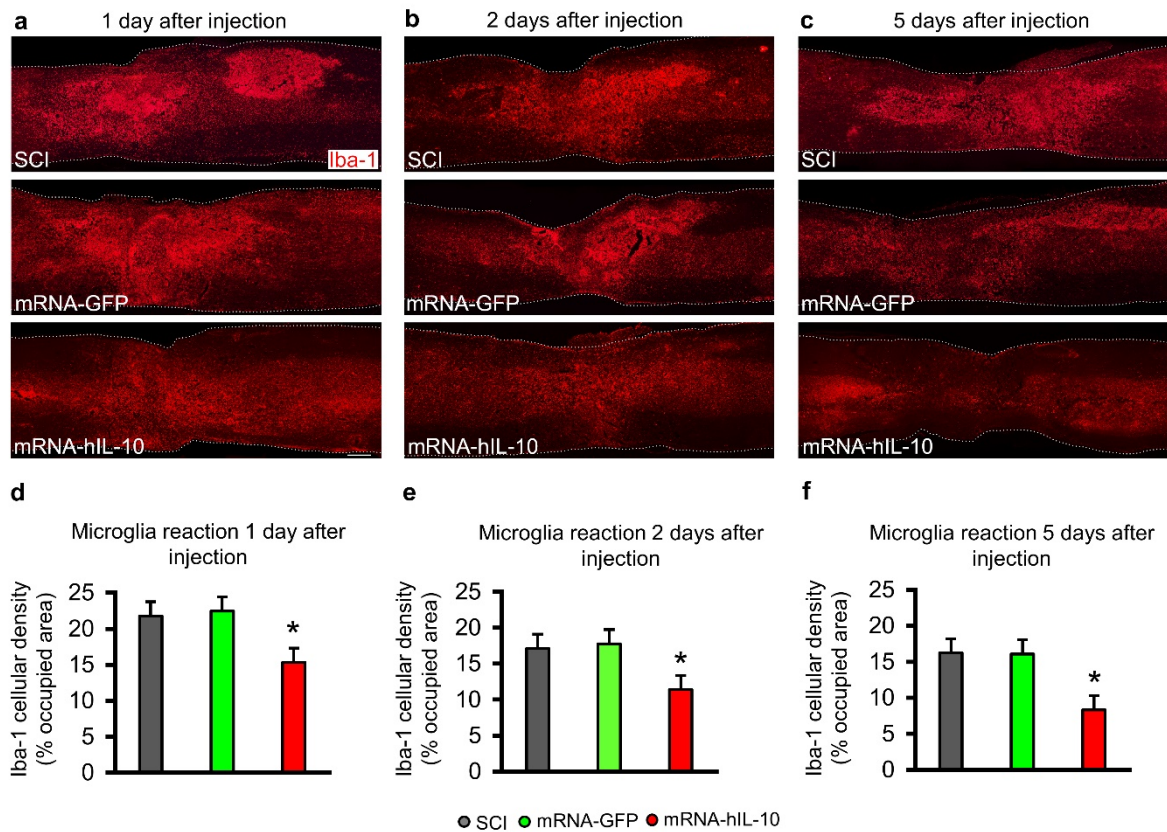
Supplementary Figure 6. hIL-10 expression in Iba-1-positive cells in the injured rat spinal cord. Images show Iba-1-positive cells co-localized with hIL-10 in injured rat spinal cord 1 day after intralésional delivery of mRNA-LNP encoding hIL-10. Scale bar: 20 μ m



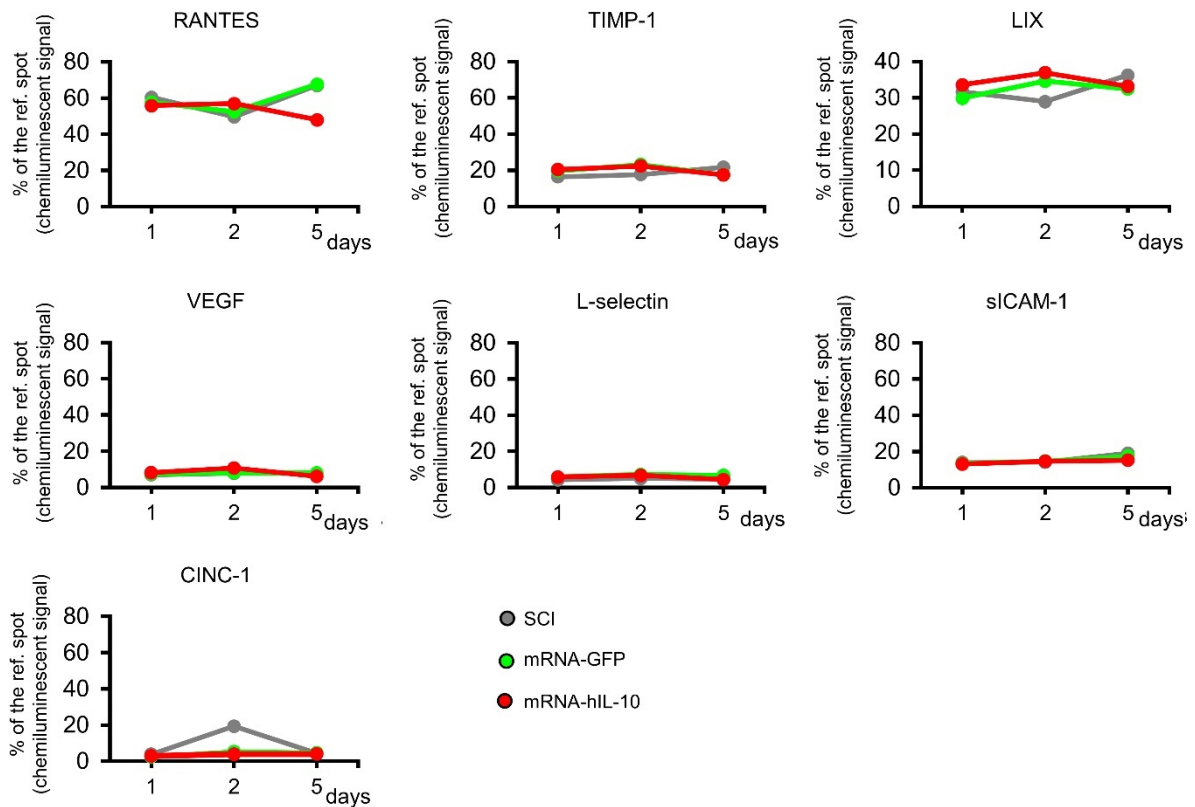
Supplementary Figure 7. hIL-10 expression in injured rat spinal cords 2 and 5 days after intralesional administration of mRNA-LNP encoding hIL-10. **a)** Confocal images show hIL-10 expression 2 days after intraspinal LNP administration in astrocytes, in GSA-B4-positive cells and in neurons. **b)** Five days after the intraspinal LNP delivery hIL-10-positive neurons and astrocytes are present in the rat spinal cord. Arrows show co-localizing cells. Scale bar in **a** 25 μm .



Supplementary Figure 8. Decreased macrophage reaction after mRNA LNP encoding hIL-10 treatment in the injured spinal cord. **a-c)** Representative images of paramedian sagittal spinal cord sections show CD68-positive cells 1, 2 and 5 days after intralesional delivery of saline (**a**), mRNA-LNP encoding eGFP (**b**) and mRNA-LNP encoding hIL-10 (**c**) in the injured spinal cord. **d-f)** Quantification of CD68 density in the sagittal sections of the spinal cord revealed significantly decreased level of CD68 at all examined time points in the hIL-10 mRNA treated group (mRNA-hIL-10) compared with the SCI and mRNA-GFP groups. Data were analysed by using one-way ANOVA with LSD multiple comparisons test. Data represent the mean \pm S.E.M. **d, e** and **f)** $n=4$, biologically independent experiments. $*p < 0.05$ indicates significant difference between SCI, mRNA-GFP vs. mRNA-hIL-10. Scale bar in **a**=300 μm .



Supplementary Figure 9. Decreased microglia reaction after mRNA LNP encoding hIL-10 treatment in the injured spinal cord. **a-c)** Representative images of paramedian sagittal spinal cord sections show Iba-1-positive cells 1, 2 and 5 days after intralesional delivery of saline (**a**), mRNA-LNP encoding eGFP (**b**) and mRNA-LNP encoding hIL-10 (**c**) in the injured spinal cord. **d-f)** Quantification of Iba-1 density in the sagittal sections of the spinal cord revealed significantly decreased level of Iba-1 expression at all examined time points in the hIL-10 mRNA treated group (mRNA-hIL-10) compared with the SCI and mRNA-GFP groups. Data were analysed by using one-way ANOVA with LSD multiple comparisons test. Data represent the mean \pm S.E.M. **d, e** and **f**) $n=4$, biologically independent experiments. $*p < 0.05$ indicates significant difference between SCI, mRNA-GFP vs. mRNA-hIL-10. Scale bar in **a**=300 μm .



Supplementary Figure 10. Circulating cytokine changes in blood serum after intralesional administration of mRNA-LNP. Rat cytokine changes were assessed with the Proteome Profiler array, which compares the relative levels of 29 cytokines. The chemiluminescent signals of spots were compared with reference spots and expressed as % of the reference spot. Abbreviations: RANTES, Regulated upon Activation, Normal T Cell Expressed and Presumably Secreted; TIMP-1, Tissue inhibitor of matrix metalloproteinase 1; LIX, Chemokine (C-X-C motif) ligand 5 (CXCL5); VEGF, Vascular endothelial growth factor; L-selectin, CD62L (a cell adhesion molecule); sICAM-1, Soluble intercellular adhesion molecule-1; CINC-1, Cytokine-induced neutrophil chemoattractant 1.

References

1. C. S. Ahuja, M. Fehlings, Concise Review: Bridging the Gap: Novel Neuroregenerative and Neuroprotective Strategies in Spinal Cord Injury. *Stem Cells Transl Med* **5**, 914-924 (2016).
2. A. Ulndreaj, A. Badner, M. G. Fehlings, Promising neuroprotective strategies for traumatic spinal cord injury with a focus on the differential effects among anatomical levels of injury. *F1000Res* **6**, 1907 (2017).
3. A. Alizadeh, S. M. Dyck, S. Karimi-Abdolrezaee, Traumatic Spinal Cord Injury: An Overview of Pathophysiology, Models and Acute Injury Mechanisms. *Front Neurol* **10**, 282 (2019).
4. X. Li *et al.*, Reactive Astroglia: Implications in Spinal Cord Injury Progression and Therapy. *Oxid Med Cell Longev* **2020**, 9494352 (2020).
5. D. R. Smith *et al.*, Polycistronic Delivery of IL-10 and NT-3 Promotes Oligodendrocyte Myelination and Functional Recovery in a Mouse Spinal Cord Injury Model. *Tissue Eng Part A* **26**, 672-682 (2020).
6. J. Park *et al.*, Local Immunomodulation with Anti-inflammatory Cytokine-Encoding Lentivirus Enhances Functional Recovery after Spinal Cord Injury. *Mol Ther* **26**, 1756-1770 (2018).
7. S. Kabu, Y. Gao, B. K. Kwon, V. Labhasetwar, Drug delivery, cell-based therapies, and tissue engineering approaches for spinal cord injury. *J Control Release* **219**, 141-154 (2015).
8. Y. Hoshino *et al.*, The adeno-associated virus rh10 vector is an effective gene transfer system for chronic spinal cord injury. *Sci Rep* **9**, 9844 (2019).
9. K. Pajer, T. Bellák, H. Redl, A. Nógrádi, Neuroectodermal Stem Cells Grafted into the Injured Spinal Cord Induce Both Axonal Regeneration and Morphological Restoration via Multiple Mechanisms. *J Neurotrauma* **36**, 2977-2990 (2019).
10. N. Pardi, M. J. Hogan, F. W. Porter, D. Weissman, mRNA vaccines - a new era in vaccinology. *Nat Rev Drug Discov* **17**, 261-279 (2018).
11. A. Magadam, K. Kaur, L. Zangi, mRNA-Based Protein Replacement Therapy for the Heart. *Mol Ther* **27**, 785-793 (2019).
12. Z. Trepotec, E. Lichtenegger, C. Plank, M. K. Aneja, C. Rudolph, Delivery of mRNA Therapeutics for the Treatment of Hepatic Diseases. *Mol Ther* **27**, 794-802 (2019).
13. I. Sahu, A. K. M. A. Haque, B. Weidensee, P. Weinmann, M. S. D. Kormann, Recent Developments in mRNA-Based Protein Supplementation Therapy to Target Lung Diseases. *Mol Ther* **27**, 803-823 (2019).
14. H. X. Zhang, Y. Zhang, H. Yin, Genome Editing with mRNA Encoding ZFN, TALEN, and Cas9. *Mol Ther* **27**, 735-746 (2019).
15. K. Karikó *et al.*, Incorporation of pseudouridine into mRNA yields superior nonimmunogenic vector with increased translational capacity and biological stability. *Mol Ther* **16**, 1833-1840 (2008).
16. K. Karikó, M. Buckstein, H. Ni, D. Weissman, Suppression of RNA recognition by Toll-like receptors: the impact of nucleoside modification and the evolutionary origin of RNA. *Immunity* **23**, 165-175 (2005).
17. N. Pardi *et al.*, Expression kinetics of nucleoside-modified mRNA delivered in lipid nanoparticles to mice by various routes. *J Control Release* **217**, 345-351 (2015).
18. D. M. Basso, M. S. Beattie, J. C. Bresnahan, A sensitive and reliable locomotor rating scale for open field testing in rats. *J Neurotrauma* **12**, 1-21 (1995).
19. D. G. Török, Z. Fekécs, K. Pajer, S. Pintér, A. Nógrádi, The use of a detailed video-based locomotor pattern analysis system to assess the functional reinnervation of denervated hind limb muscles. *J Neurosci Methods* **365**, 109398 (2022).

20. D. J. Hellenbrand *et al.*, Sustained interleukin-10 delivery reduces inflammation and improves motor function after spinal cord injury. *J Neuroinflammation* **16**, 93 (2019).
21. A. R. Burmeister, I. Marriott, The Interleukin-10 Family of Cytokines and Their Role in the CNS. *Front Cell Neurosci* **12**, 458 (2018).
22. F. P. Polack *et al.*, Safety and Efficacy of the BNT162b2 mRNA Covid-19 Vaccine. *N Engl J Med* **383**, 2603-2615 (2020).
23. L. R. Baden *et al.*, Efficacy and Safety of the mRNA-1273 SARS-CoV-2 Vaccine. *N Engl J Med* **384**, 403-416 (2021).
24. K. L. Brewer, J. R. Bethea, R. P. Yeziarski, Neuroprotective effects of interleukin-10 following excitotoxic spinal cord injury. *Exp Neurol* **159**, 484-493 (1999).
25. T. H. Tran, R. Rastogi, J. Shelke, M. M. Amiji, Modulation of Macrophage Functional Polarity towards Anti-Inflammatory Phenotype with Plasmid DNA Delivery in CD44 Targeting Hyaluronic Acid Nanoparticles. *Sci Rep* **5**, 16632 (2015).
26. W. D. Whetstone, J. Y. Hsu, M. Eisenberg, Z. Werb, L. J. Noble-Haeusslein, Blood-spinal cord barrier after spinal cord injury: relation to revascularization and wound healing. *J Neurosci Res* **74**, 227-239 (2003).
27. X. Wu *et al.*, Cytokine-induced neutrophil chemoattractant mediates neutrophil influx in immune complex glomerulonephritis in rat. *J Clin Invest* **94**, 337-344 (1994).
28. Y. Ohta *et al.*, Intravenous infusion of adipose-derived stem/stromal cells improves functional recovery of rats with spinal cord injury. *Cytotherapy* **19**, 839-848 (2017).
29. J. Tang, Y. Kang, L. Huang, L. Wu, Y. Peng, TIMP1 preserves the blood-brain barrier through interacting with CD63/integrin. *Acta Pharm Sin B* **10**, 987-1003 (2020).
30. E. Tejima *et al.*, Neuroprotective effects of overexpressing tissue inhibitor of metalloproteinase TIMP-1. *J Neurotrauma* **26**, 1935-1941 (2009).
31. S. J. Crocker *et al.*, Persistent macrophage/microglial activation and myelin disruption after experimental autoimmune encephalomyelitis in tissue inhibitor of metalloproteinase-1-deficient mice. *Am J Pathol* **169**, 2104-2116 (2006).
32. M. Fang *et al.*, Antineuroinflammatory and neurotrophic effects of CNTF and C16 peptide in an acute experimental autoimmune encephalomyelitis rat model. *Front Neuroanat* **7**, 44 (2013).
33. Q. Cao *et al.*, Transplantation of ciliary neurotrophic factor-expressing adult oligodendrocyte precursor cells promotes remyelination and functional recovery after spinal cord injury. *J Neurosci* **30**, 2989-3001 (2010).
34. N. G. Carlson *et al.*, Inflammatory cytokines IL-1 alpha, IL-1 beta, IL-6, and TNF-alpha impart neuroprotection to an excitotoxin through distinct pathways. *J Immunol* **163**, 3963-3968 (1999).
35. A. W. Freyn *et al.*, A Multi-Targeting, Nucleoside-Modified mRNA Influenza Virus Vaccine Provides Broad Protection in Mice. *Mol Ther* **28**, 1569-1584 (2020).
36. M. Baiersdörfer *et al.*, A Facile Method for the Removal of dsRNA Contaminant from In Vitro-Transcribed mRNA. *Mol Ther Nucleic Acids* **15**, 26-35 (2019).
37. M. A. Maier *et al.*, Biodegradable lipids enabling rapidly eliminated lipid nanoparticles for systemic delivery of RNAi therapeutics. *Mol Ther* **21**, 1570-1578 (2013).
38. T. Bellák *et al.*, Grafted human induced pluripotent stem cells improve the outcome of spinal cord injury: modulation of the lesion microenvironment. *Sci Rep* **10**, 22414 (2020).
39. A. Arevalo-Martin *et al.*, Early endogenous activation of CB1 and CB2 receptors after spinal cord injury is a protective response involved in spontaneous recovery. *PLoS One* **7**, e49057 (2012).